ELECTRONIC SUPPLEMENTARY MATERIALS
for

A new giant titanosaur sheds light on body mass evolution amongst sauropod dinosaurs

José L. Carballido*[1], Diego Pol[1], Alejandro Otero[2], Ignacio A. Cerda[3], Leonardo Salgado[3], Alberto C. Garrido[4], Jahandar Ramezani[5], Néstor R. Cúneo[1], Javier M. Krause[1].

[1]*CONICET, Museo Paleontológico Egidio Feruglio, Trelew U9100GYO, Argentina.* jcarballido@mef.org.ar
[2]*CONICET, División Paleontología de Vertebrados, Museo de La Plata, La Plata B1900FWA, Argentina.*
[3]*CONICET, Instituto de Investigación en Paleobiología y Geología, Universidad Nacional de Río Negro, General Roca 8332, Argentina.*
[4]*Museo Provincial de Ciencias Naturales "Juan Olsacher",Zapala 8340, Argentina., Argentina.*
[5]*Department of Earth, Atmospheric and Planetary Sciences, Massachusetts Institute of Technology, Cambridge, MA 02139, USA.*

Proceedings of the Royal Society B

DOI: 10.1098/rspb.2017.1219

This file includes:

1. Materials and Methods

1.1 Taphonomy

Collection history

The rural farmer Aurelio Hernandez originally recognized the first fossils found at the site of *Patagotitan mayorum* in 2010, at "La Flecha" Farm owned by the Mayo family. The finding was reported to P. Puerta, from the Museo Paleontológico Egidio Feruglio (MPEF) and in 2012 a preliminary field expedition was carried out to the La Flecha farm. A few weeks later (January 2013), a subsequent expedition was carried out and the first elements were uncovered and collected, including the largest femur (MPEF-PV 3399/44) and a pubis (MPEF-PV 3399/40-4). Between January 2013 and February 2015 seven paleontological field expeditions were carried out to the La Flecha fossil site, recovering more than 200 fossils, including almost 130 sauropod bones and 57 theropod teeth. All of the sauropod materials are here attributed to Patagotitan mayorum and all of them comes from the same quarry (La Flecha; FLV), but from three different layers named FLV1, FLV2, and FLV3 (see below; Fig. S1 and Fig. S2). A second small quarry (FLV4) was opened at the same level but 300 meters west from the original one. At this place a similar sized sauropod, consisted of eight articulated caudal vertebrae with their chevrons in anatomical position and two pubes, was uncovered but not collected yet. Precise GPS locations of the sites are deposited at MPEF collection and can be obtained upon request.

Description of the "La Flecha" quarry

The quarry exhibits a monotonous succession of interbedded muddy sandstones and sandy mudstones, with thin intercalations of fine-grained sandstone and tuffaceous beds. The front of the quarry reaches 3.43 m high and bones were found in three distinct but closely spaced horizons. The first bone level (0.40 m thick; FLV1) contains remains of a partially associated individual (MPEF-PV 3399; Fig. S1) and isolated bones that belong to at least two other slightly smaller individuals (approximately 80-90%). The isolated remains include two fragmentary fibulae of different size (MPEF-PV 3391; MPEF-PV 3392), two humeri (MPEF-PV 3395, MPEF-PV 3396), a femur (MPEF-PV 3394), a cervical centrum (MPEF-PV 3390), and more fragmentary remains. The second bone level (0.30 m thick; FLV2; Fig. S1) is placed 1 m above the first and contains limited material (three isolated skeletal remains, a humerus [MPEF-PV 3397] and fragmentary dorsal ribs). Finally, the third level (0.35 m thick; FLV3; Fig. S1) is situated 0.40 m above the second level and includes the holotype specimen (MPEF-PV 3400) and other scattered bones of, at least, one more individual. These include a third femur from this level (MPEF-PV 3394) that has signs of trampling on its proximal end, which was crushed.

The bearing sediments indicates that sedimentation took place with a low energy setting, related to floodplains of a meandering system (Carmona et al., 2016). The degree of disarticulation of the bones, as well as their different modes of preservation, suggest a prolonged subaerial exposure of the specimens, especially those found as isolated bones. Those levels clearly represent three distinct moments of death (FLV1, FLV2 and FLV3), however, there are also differences of preservation and stage of weathering among the individuals recovered within FLV1 (with a Minimum Number of Individuals (MNI) of 3)

and among those recovered within FLV3 (MNI=2). These differences are interpreted as caused by different times in subaerial exposure of the individuals before they were covered by the flooding episodes. A brief description of the elements and preservations of the individuals recovered in the three levels is here provided.

In FLV1 most of the bones are attributed to a single individual (MPEF-PV 3399) accumulated in two slightly spaced clusters of bones (Fig. S1). One of these clusters is composed by three posterior dorsal vertebrae, one ulna and one radius (closely found one from each other), two pubes and two ischia, one femur, partially preserved anterior and middle caudal centra, chevrons, and ribs. The second cluster assigned to the individual MPEF-PV 3399 is composed by the posteriormost cervical vertebrae and cervical ribs. Additional specimens from FLV1 are represented by isolated bones, including two partially preserved fibulae (of different sizes), two left humeri (both of them having their proximal and distal sections poorly preserved), an almost complete femur (smaller than the one from MPEF-PV 3399), a weathered cervical centrum, and scattered material including some broken ribs and fragments of caudal vertebrae. Therefore, whereas the individual MPEF-PV 3399 is well preserved and with closely associated body elements, remaining specimens are represented by heavily weathered bones (e.g. the fibulae and humeri). Although we cannot completely discard that some of them actually belong to the individual MPEF-PV 3399 (e.g., one of the two humeri or fibulae), the other bones must pertain to a second and third individuals preserved within FLV1, the isolated femur (MPEF-PV 3394), which is smaller than that of MPEF-PV 3399, and one of the almost equally sized right humerii (MPEF-PV 3395-3396) must represent the second and third individuals.

The single specimen recovered from FLV2 (the intermediate level) is an isolated right humerus (MPEF-PV 3397) and uncollected rib fragments. The humerus is well preserved and is the largest humerus recovered in the quarry.

The MNI from FLV3 is two. One of the individuals is extremely well preserved, with articulated and closely associated elements (Fig. S1). This specimen (MPEF-PV 3400) was selected as the holotype due to its extremely good preservation and presence of autapomorphic characters diagnosing the species. The holotype is composed by two anterior cervical vertebrae, a series of eight dorsal vertebrae, the anteriormost caudal vertebrae, a scapula and coracoid, two sternal plates, two pubes, two femora, ribs, and chevrons. Some of the bones from this individual were in natural articulation, such as three anterior caudals (C3-C-5) with their respective chevrons (identified as the first and second chevron), whereas others were closely associated but not in natural articulation (e.g., the coracoid and the scapula, the two sternal plates, pubes, femora). A third femur recovered from this level represents the second specimen found at FLV3. The third femur recovered from this level is badly preserved and with signs of trampling on its proximal region.

Environment

The low energy depositional setting indicates that the specimens were not transported by flows prior to their burial. The heterolithic facies, fine-grained sandstones, and tuffaceous siltstones constituting the La Flecha quarry, were interpreted as deposited during sporadic flood episodes through sheet floods and settling from suspension within a floodplain environment (Carmona et al., 2016). In all cases, the estimated flow energy

was insufficient to enable the transport or displacement of large bones found in the three fossiliferous horizons. Therefore, mechanical transport can be discarded as a hypothesis of the accumulation found at La Flecha quarry.

Evidence for the monospecificity of the site

The presence of repeated elements between the different specimens, especially between the most complete individulas (MPEF-PV 3400 and MPEF-PV 3399), allows us to compare and recognize the site as a monospecific assemblage. Repeated and isolated elements do not have anatomical difference between them, even coming from different levels.

Dorsal vertebrae are preserved for both, MPEF-PV 3400 and MPEF-PV 3399. The morphology and size of these elements does not show any morphological difference more than those related to serial variations. Even more, two elements are here interpreted as coming from the same position of the dorsal series (dorsal 3). The third dorsal, preserved for this two specimens, presents the parapophysis at the same position (right above the dorsal centrum), and both luck hypantrum but have a well developed triangular hyposphene below the postzygapophysis. Taking into account the absence of hyposphene and hypantrum in all the other preserved dorsal vertebrae (from the middle to the posterior region) we interpreted this as a unique character of *Patagotitan*. Therefore these two specimens share the same unique character in the dorsal series. An anterior caudal vertebra, identified as the first caudal, was recovered for both specimens. Both caudals are nearly identical but for preservation and minors differences. These caudals also share autapomorphic characters, the flat anterior articular surface and the strongly convex posterior one, and the wider neural spines with the incipiently bifid dorsal margin and the anteriorly directed tips. The femur is also a repeated element between these two specimens, having slight differences of size but the same morphology, including the straight lateral edge. No humerus was recovered for these specimens, but three humeri were recovered from the site, two of them coming form FLV1 and one from FLV2. These three humeri, besides general morphology and proportions also share the presence of a marked bulge on the posterolateral surface. With the evidence at hand we consider that all the sauropod specimens are from the same species and therefore identifying the association as monospecific.

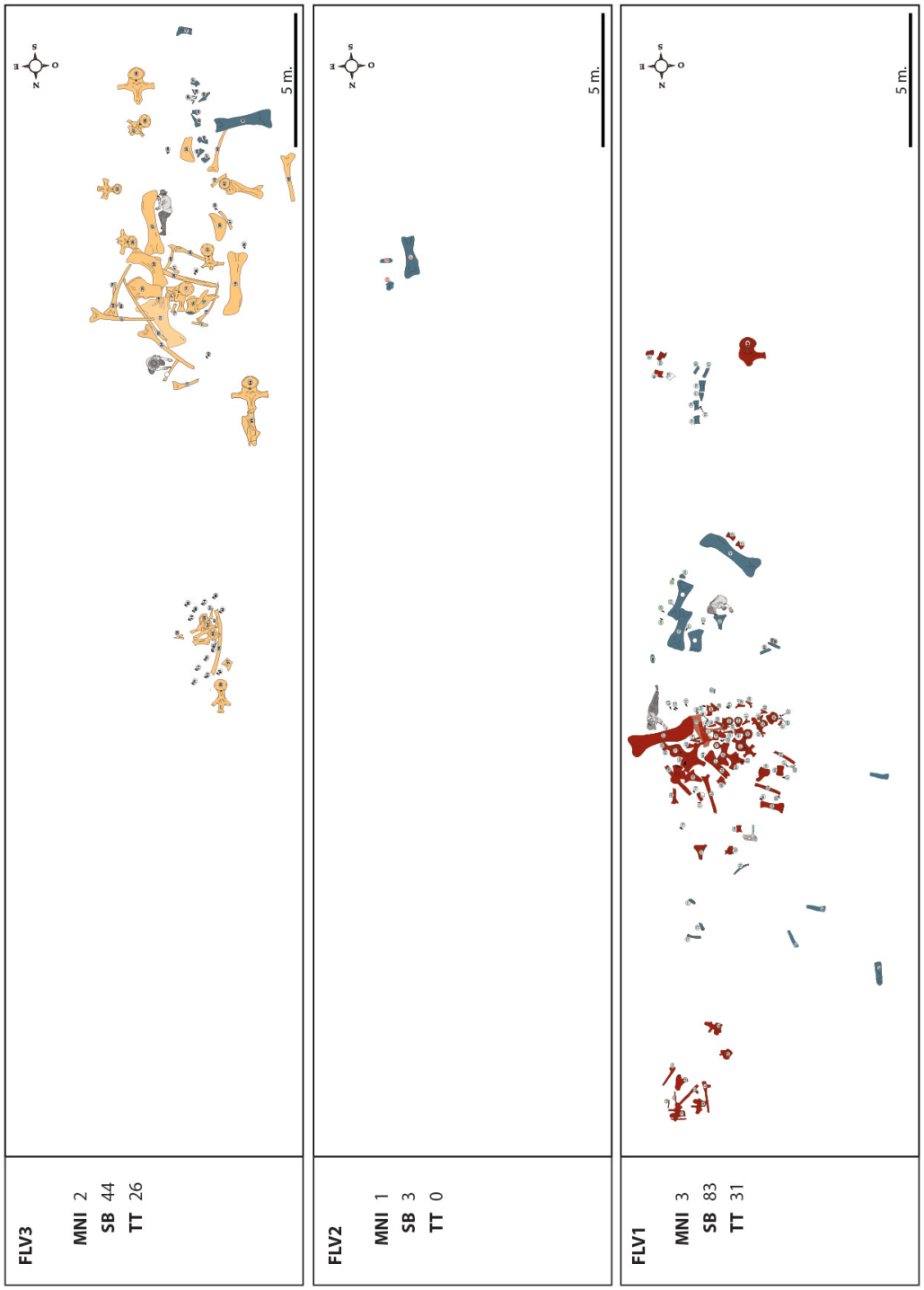

Fig. S1. Taphonomic map of the "La Flecha" quarry showing the different levels and specimens. **FLV1**. Red bones represnets the most complete individual (MPEF-PV 3399), and green bones are thos that representes further specimens (at least 2). **FLV2**. Green bones are atrributed to a single specimen, but solely the humerus was collected. **FLV3**. Yelow bones are thos of the most complete specimen recovered from that level, which represents the holotype. Green femur is representin the second pecimen at that level. **Abreviations**: **MMN**, Minimal Number of Individuals; **SB**, Sauropod Bones; **TT**, Theropod Teeth.

Fig. S2. Complete taphonomic map of the “La Flecha” quarry (FLV1. FLV2, and FLV3).

1.2 U-Pb Geochronology

Sample and methods

A sample of tuffaceous siltstone from the La Flecha Quarry was collected for radioisotopic dating in order to constrain the depositional age of the fossil-bearing layers. Sample Cenizo-P was collected from the interval between bone layers FLV1 and FLV2 (30 cm above FLV1), ~4.5 meters below the base of the Las Plumas Member of the Cerro Barcino Formation. Zircons separated from sample Cenizo-P were analyzed by the U–Pb isotope dilution thermal-ionization mass spectrometry (ID-TIMS) technique following the detailed procedures described in Ramezani et al. (2011). Single zircon grains were pre-treated by a chemical abrasion (CA-TIMS) method modified after Mattinson (2005) to mitigate the effects of radiation-induced Pb loss, and were spiked with the EARTHTIME ET535 mixed ^{205}Pb–^{233}U–^{235}U tracer (Condon et al., 2015; McLean et al., 2015) before complete acid digestion and analysis. Isotopic measurements of Pb and U were made on a Sector 54 multi-collector mass spectrometer equipped with a Daly ion counting system at the MIT Isotope Laboratory. Reduction of U–Pb isotopic data including date calculation and propagation of uncertainties was carried out using computer applications and algorithms of Bowring et al. (2011) and McLean et al. (2011). Complete U–Pb data appear in the supplementary material Table S1.

Tuffaceous (volcaniclastic) sedimentary deposits, particularly those in continental fluvial settings, commonly contain reworked or detrital materials from older source rocks that complicate determination of the true depositional age. Multiple (>10) high-precision analyses are often needed to resolve distinct zircon age populations. The sample date is calculated based on the weighted mean ^{206}Pb/^{238}U date of a statistically coherent cluster of the youngest zircon analyses from the sample provided that there are at least 3 analyses in the cluster. In the absence of other stratigraphic age constraints, the above weighted mean date is interpreted as the maximum age of deposition.

Date uncertainties are reported at 95% confidence level and follow the notation $\pm X/Y/Z$ Ma, where X is the internal (analytical) uncertainty in the absence of all external errors, Y incorporates the U–Pb tracer calibration error and Z includes the latter as well as the U decay constant errors of Jaffey et al. (1971). Complete uncertainties (Z) must be taken into account for comparison between age data from different isotopic chronometers (e.g. U–Pb versus ^{40}Ar/^{39}Ar).

Results and age interpretation

Selected zircons for analysis were multi-faceted prisms, mostly with visible glass (melt) inclusions and no detectable evidence of abrasion or rounding (supplementary material Figure S3A). Thirteen zircon analyses from sample Cenizo-P ranged in ^{206}Pb/^{238}U date from 313.84 ± 0.19 Ma to 101.55 ± 0.18 Ma. The three youngest analyses form a coherent cluster with a weighted mean ^{206}Pb/^{238}U date of 101.62 ± 0.11/0.14/0.18 Ma and a mean square of weighted deviates (MSWD) of 0.57 (Table S1 and Figure S3B).

The above measured date that coincides with the late Albian (latest Early Cretaceous) based on the GTS2012 time scale (Ogg and Hinnov, 2012) serves as the best estimate for the maximum age of deposition of the bone layers in the La Flecha Quarry. It is also consistent with the U-Pb CA-TIMS zircon geochronology from the middle and lower intervals of the Cerro Castaño Member of the Cerro Barcino Formation (Krause et al., in prep.), as well as the pre-late Cenomanian minimum age of the uppermost Chubut

Group based on SHRIMP U-Pb geochronology (Suárez et al., 2014). It can thus be postulated that our measured date of 101.62 ± 0.18 Ma is fairly close to the true depositional age of the Cerro Castaño Member strata exposed at the La Flecha Quarry. Nevertheless, our limited age data cannot rule out the possibility that the true depositional age of the La Flecha bone layers could be early Late Cretaceous instead. Tighter age constraints on the bone layers await more extensive geochronologic work that is currently in progress.

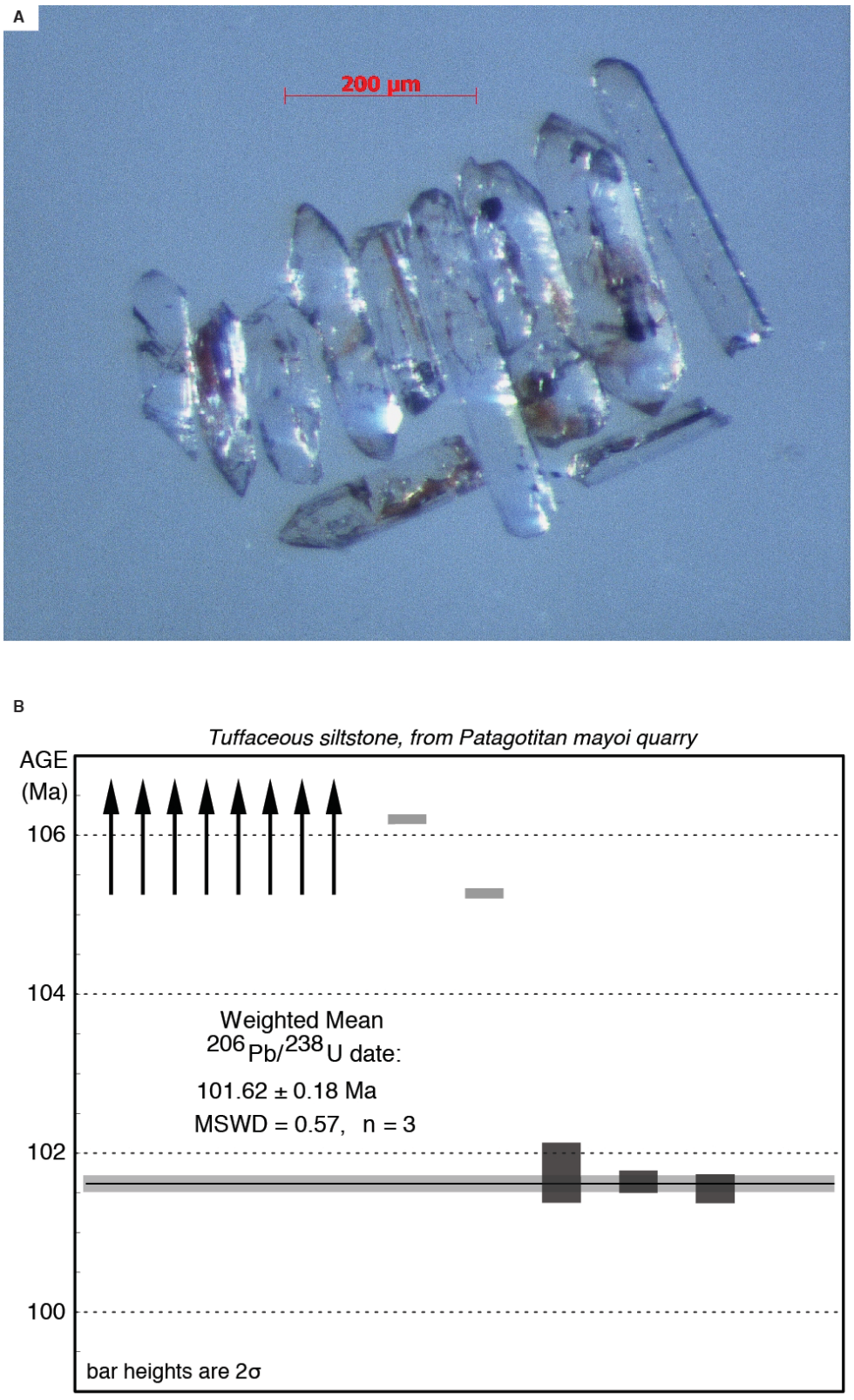

Fig. S3. A) Microscope image of analysed zircon from sample Cenizo-P, La Flecha Quarry, Chubut, Argentina. B) Date distribution plot of analysed zircons of this study. Bar heights are proportional to 2σ

analytical uncertainty of individual analyses; solid bars are analyses used in age calculation. Horizontal line signify calculated sample dates and the width of the shaded band represents internal uncertainty in weighted mean at 95% confidence level. Arrows points to additional analyses plotting outside the diagram. Reported date incorporates all sources of uncertainty.

1.3. Bone histology

Petrographic thin sections of *Patagotitan* long bones (five femora and one humerus) were prepared from five individuals, including the femora of the holotype (MEPF-PV 3400/27, MPEF-PV 3400/26) and paratypes (MPEF-PV 3375; MPEF-PV 3394; MPEF-PV 3397; MPEF-PV 3399/44). The results were used to estimate the developmental stage of each specimen. In addition we used histological examination to infer whether the heavily striated external texture of the transverse process and the tip of the neural spine in anterior caudal vertebrae had a histological signature of a strong ligament/tendinous attachment. For this, we studied a cross section obtained from the transverse process of a second caudal vertebra (MPEF-PV 3400/17) and longitudinal and transversal sections from the tip of a first caudal vertebra (MPEF-PV 3400/11).

Specimens were prepared for thin sections based on the methodology outlined in Chinsamy and Raath (1992). The preparation of the histological sections was carried out at the Museo Paleontológico Egidio Feruglio (Trelew, Argentina). The thin sections were studied using petrographic polarizing microscope (Nikon E400). Nomenclature and definitions of structures used in this study are derived from Francillon-Vieillot et al. (1990) and Chinsamy-Turan (2005).

Long bone histology.

Since that long bones share general histological features, we describe them together. The compacta is mostly composed of dense Haversian bone (Fig. S4A, B). Secondary osteons of more than one single generation are observed in the inner cortex. In this area, Haversian canals appear to be larger, which indicates that they are in an early stage of development. Remains of primary bone are observed in the upper most portion of the cortex. Primary bone consists of well vascularized fibro-lamellar bone tissue (Fig. S4C). Primary osteons are mostly longitudinally oriented and they are arranged in concentric laminae. Short circumferential and radial vascular spaces are also observed, but they are much less abundant. Osteocyte lacunae are rounded or slightly elongated in shape. Fibro-lamellar bone is interrupted by closely spaced lines of arrested growth (LAGs), which can be single or double (Fig. S4C). At least seven LAGs where observed in the specimen MPVEF 3399/44. There is not important changes in the intrinsic fiber orientation and vascular spaces density in the outer cortex.

The presence of dense Haversian bone and substantially diminished spacing between LAGs near the sub-periosteal surface indicates that all the studied individuals were somatically mature and they died during a phase of slow-down growth rate (Klein and Sander 2008). However, the absence of an Outer Circumferential Layer (i.e. layer of avascular lamellar or parallel-fibered bone with tightly spaced LAGs, Chinsamy Turan 2005) in the sampled specimens reveals that they were still growing individuals.

Vertebral histology

The wing-like transverse process of a partially preserved second caudal vertebrae exhibits a highly pneumatized internal structure (camellate *sensu* Wedel et al., 2000), which consists of thick trabeculae (1-5 mm) enclosing small spaces of irregular shape (Fig. S4F). Osseous trabecuale are partially or entirely coated by lamellar bone tissue deposited during different generations of bone remodeling. The trabecuale are internally composed of dense Haversian bone tissue (Fig. S4G). The cortical tissue is thin (equals or

even thinner than some bony trabeculae) and is mostly composed of secondary bone tissue. Haversian osteons exhibit variable shape, size and orientation, and they are communicated by several Volkmann's canals (Fig. S4H). Remains of primary bone are observed in the outermost portion of the cortex. This bone appears to be mostly avascular and contains abundant Sharpey's fibers (Fig. S4I). Growth marks are also discernible in primary bone. Unfortunately the poor preservation of the outer cortex precludes a more detailed characterization of the primary bone tissue.

Regarding the tips of the neural spines of the anterior caudal vertebrae, the bone tissue is mainly composed of secondary osteons of different generations and in different stages of development (Fig. S4J). Volkmann canals occasionally connect the Haversian systems. Primary bone consists of an avascular tissue formed by coarse bundles of mineralized collagenous fibers (Fig. S4K). These fibers are mostly longitudinally arranged (i.e. parallel to the main body axis), but some variation can occur in some regions. Bone cell lacunae are not clearly discernible in the primary bone.

The histological data obtained from both the transverse process and neural spine tip of the anterior caudal vertebra supports the inferences obtained from macroscopic observations. In this sense, the mineralized fibers observed in the neural spine sections appear to correspond with metaplastic ossification from an interspinous or supraspinous ligament inserted in this area. In the case of the abundant Sharpey's fibers recognized in the transverse process, this histological feature also is congruent with a strong muscle attachment in this area.

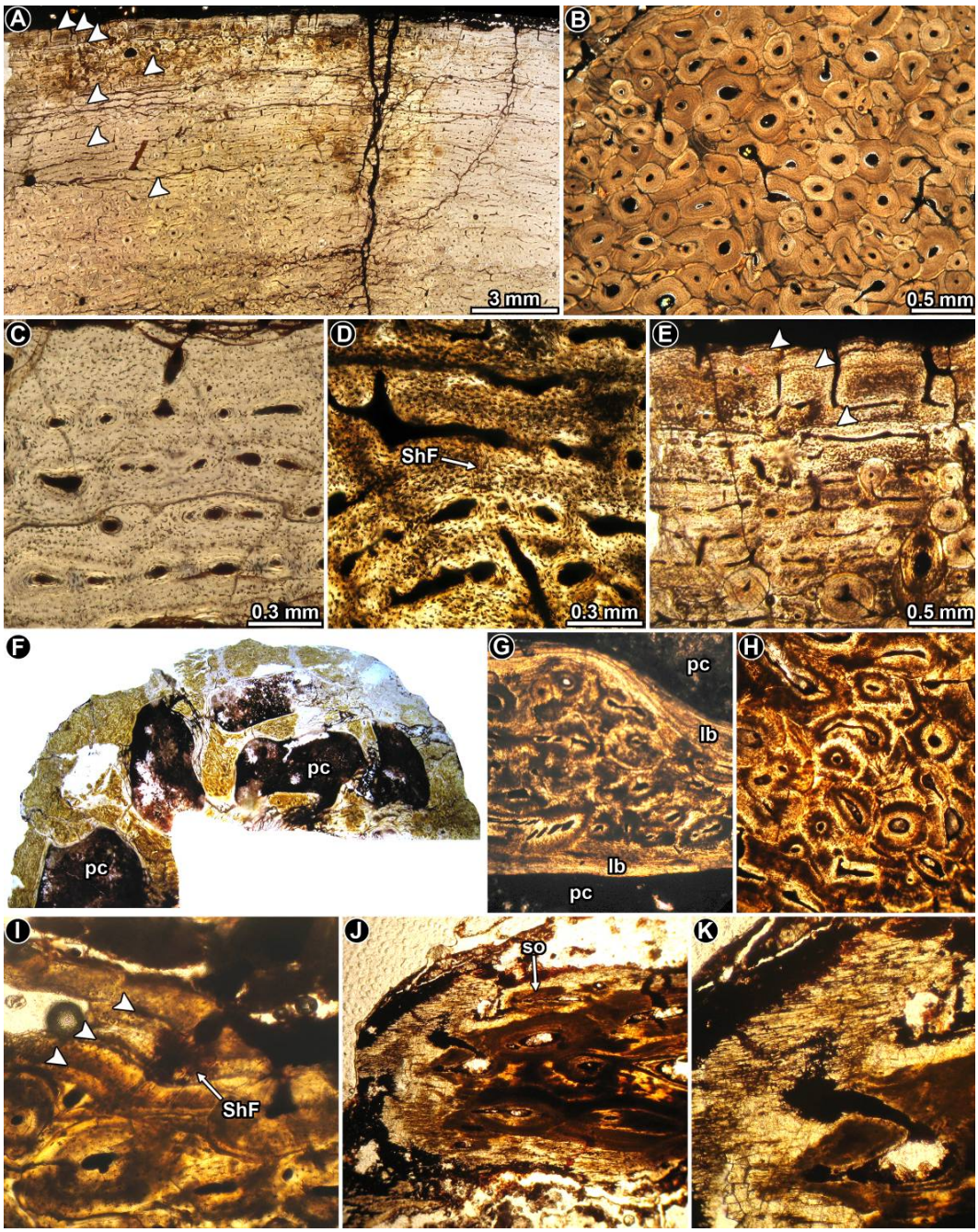

Fig. S4. Long bones histology of *Patagotitan mayorun* (**A-E**), caudal transverse process (**F-I**) and caudal neural spine (**J, K**). A, general view of the outer cortex of MPVEF 3399/44. Arrowheads denote the presence of lines of arrested growth (LAGs). B, dense Haversian bone tissue in the mid cortex of MPVEF 3399/44. **C, D**, detailed view of fibrolamellar bone in the outer cortex. **E**, Note the presence of several double lines of arrested growth (arrowheads) at the subperiosteal cortex. **F**, cross section of transverse process showing abundant pneumatic cavities and a thin cortex. **G**, detailed view of a internal trabecula composed of dense Haversian bone and coated by lamellar bone tissue. **H**, enlarged view of the dense Haversian bone of the cortex. **I**, remains of primary bone tissue at the outermost cortex showing several Sharpey's fibers. Arrowheads denote growth marks. **J**, longitudinal section of the neural spine tip showing both secondary osteons and primary bone tissue. **K**, detail of same picture showing dense fibrous primary bone tissue. **Abbreviations**: **lb:** lamellar bone; **pn:** pneumatic cavity; **ShF:** Sharpey's fibers; **so:** secondary osteons.

1.2 Body mass

Body mass estimation

Based on the available remains we have conducted two alternative methods of body mass estimations for *Patagotitan mayorum*: long bone circumference (Campione and Evans, 2012) and volumetric reconstruction (Sellers et al., 2012).

Long bone circumference. The first method for body mass calculation implemented here was based on long bone circumferences. This method was first proposed by Anderson (1985) and considers the body mass as a function of the circumference of either femur (for biped animals) or femur + humerus (for quadrupedal animals). We used the modification implemented by Campione and Evans (2012), which uses a scaling equation, adjusted for phylogenetic correlation/covariance between species, as follows: Log BM = 2.749 . log (CH+CF) - 1.104. Using this methodology (see Table S5 for measurements) the body mass estimated for *Patagotitan* is of 69.092 tons, and between 51.819 and 86.365 tons when the mean percent prediction error (PEE) is taking into account. The body mass estimation is much larger than the estimates given by Benson et al. (2014) for *Apatosaurus louisae* (41.268 tons), *Giraffatitan* (34.003 tons), *Alamosaurus* (35.163), and *Futalonkgosaurus* (38.138), and also larger than that of *Dreadgnothus* (59.290) (Lacovara et al., 2014). Based on the scaling equation of Campione and Evans (2012) the body mass estimates of these large sauropods ranges from 49% to 85% of that obtained for *Patagotitan mayorum*. Applying this scaling approach to the giant sauropods *Argentinosaurus* and *Puertasaurus* is problematic or impossible, as discussed below.

Volumetric reconstruction.

This approach, using a convex hull method (based on a reconstructed complete skeleton), was used to estimate the body volume of *Patagotitan mayorum*. This method has been previously implemented for different sauropod taxa (Sellers et al., 2012; Bates et al., 2015, 2016) based on 3D skeletal models. Here we used a digital reconstruction of the skeleton of *Patagotitan* based on surface scans of preserved elements and completing the skeleton with reconstructed 3D elements. The skeletal model was imported as an .obj file into MeshLab (Visual Computing Lab – ISTI – CNR; http://meshlab.sourceforge.net/). Following the protocol of Sellers et al. (2012) the 3D model was divided into body segments, as follows: head, neck, trunk, tail, humerus, radius + ulna, carpus+ manus, femur, tibia+fibula, and tarsus+pes. Also, the model was set in a reference pose with neck and tail horizontally positioned and limbs fully extended (Fig. S5). A minimum convex hull was calculated for each segment; hence a minimum volume estimate is calculated for the entire animal. As the mass estimations through volume require density as a variable, a density of 1000 kg m^3 was used for the mass calculation (Alexander, 1989; Sellers et al., 2012; Bates et al., 2015, 2016). Respiratory structures were calculated and included in the minimum convex hull estimation here reported (Table S2), giving a new density for the whole skeleton (Table S2). Maximal model and 21% expanded convex hull volume were calculated as well (Table S2) following the same protocol described by Sellers et al (2012). Using the minimum convex hull model, the estimated body mass for *Patagotitan* is 44.21 tons. This is 64% the mass estimated by the scaling method based on long bone circumference (Campione

and Evans, 2012) and is consistent with previous findings that noted disparities between the scaling and the volumetric approaches for dinosaur body mass estimations (Bates et al., 2015). As with the scalling equations, the 44.21 tons depicted for *Patagotitan* (obtained with the minimum convex hull reconstruction) is larger than the minimum convex hull volumetric body mass estimated for other large sauropods such as *Giraffatitan* (25.28 tons) and *Dreadgnothus* (26.91 tons) or *Apatosaurus* (26.63 tons) (Benson et al., 2014; Bates et al., 2015). The volumetric estimates of these sauropods therefore range between 57% and 60% of the body mass estimation here made for *Patagotitan*.

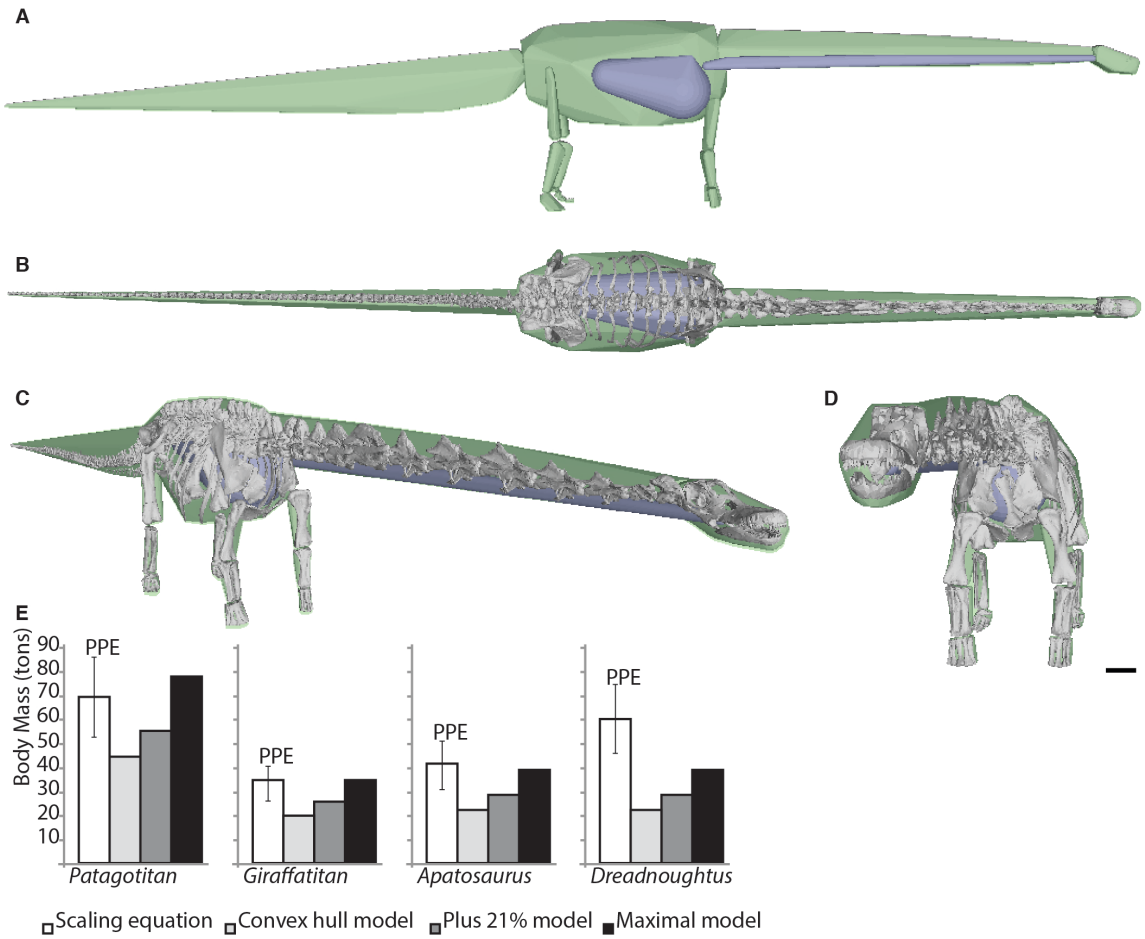

Fig. S5. Convex hull model made for calculating the body volume of *Patagotitan mayorum*, in A, left lateral and; B, dorsal, C, right anterolateral; and D, left anterior views. E, mass predictions from the different models (*Giraffatitan*, *Apatosaurus* and *Dreadnoughtus* after Bates et al., 2015).

Table S2. Volumetric Body Mass reconstruction based on convex hull reconstructions made for *Patagotitan*.

BODY SEGMENTS	Volume (m3)	Density	Mass (Kg)
Head	0.13	1000	130
Neck	7.02	1000	7020
Trunck	35.63	1000	35630
Tail	6.1	1000	6100
Humerus	0.23 (x2)	1000	230 (x2)
Forearm	0.15 (x2)	1000	150 (x2)
Hand	0.08 (x2)	1000	8 (x2)
Thigh	0.43 (x2)	1000	430 (x2)
Shank	0.19 (x2)	1000	190 (x2)
Foot	0.07 (x2)	1000	70 (x2)
Hind Limb Total	0.46 (x2)	1000	460 (x2)
Fore Limb Total	0.69 (x2)	1000	690 (x2)
Whole Body (WB)	51.18	1000	51180

RESPIRATORY STRUCTURES			
Neck	0.85	1000	-850
Trunk	6.12	1000	-6112
Total air structures	6.97	1000	-6970
MODEL ITERATION			
Minimum convex hull	51.18	863.81	**44210**
Plus 21% model	61.92	887.44	**54957**
Maximal model	84.54	917.55	**77570**

The problem of body mass estimation for *other giant titanosaurs*

Argentinosaurus huinculensis has been considered the largest valid dinosaur genus during the last decades (Mazzetta et al., 2004; Benson et al., 2014). This taxon, however, is known from fragmentary remains, and therefore, quantitative methods for body mass estimation cannot be directly applied. The holotype material of *Argentinosaurus* includes six dorsal vertebrae, a partial sacrum, a fibula and a dorsal rib (Bonaparte and Coria, 1991). The fragmentary nature of the type specimen precludes a whole-skeleton volumetric approach such as the one described above, and the absence of femur and humerus prevents applying the scaling equations proposed by other authors (e.g., Campione and Evans, 2012). Despite these problems, two previous studies (Mazzetta et al., 2004; Benson et al., 2014) estimated the body mass of *Argentinosaurus* by applying scaling equations and measurements taken from two isolated femoral shafts found in deposits of the Huincul Formation. Clearly, none of them can be referred to *Argentinosaurus huinculensis* given the complete absence of femoral remains in the type material. One of these fragmentary femora is housed at the Museo de La Plata collection (MLP-DP- 46-VIII-21-3) whereas the other femoral remain (partially reconstructed with plaster) is housed at the Museo Municipal "Carmen Funes".

Benson et al. (2014) estimated the body mass of multiple species of dinosaurs using the same equations of Campione and Evans (2012) and that we implemented in this contribution (see above). For *Argentinosaurus*, Benson et al. (2014) used the circumference of the fragmentary and partially reconstructed isolated femur housed at the Museo Municipal "Carmen Funes" and used a hypothetical humeral circumference predicted by a least-square regression between humeral and femoral circumferences. This procedure yielded a 95% confidence interval for the body mass ranging from 67 to 124 tons. Personal observation on this isolated femur (that comes from the same unit than *Argentinosaurus*) showed us that most of it is reconstructed with plaster, and therefore this measure cannot be confidently used. Additionally, due to the absence of femur in the holotype of *Argentinosaurs* the isolated femur cannot confidently be used for estimating the body mass of *Argentinosaurus*.

Mazzetta et al. (2004) used a different scaling equation that only needs the femoral circumference and under this procedure they measured the other isolated femoral shaft collected from the Huincul Formation and housed at the Museo de La Plata collection (MLP-DP- 46-VIII-21-3). This femoral shaft is better preserved than the one at the Museo Municipal "Carmen Funes" and its circumference can be confidently measured, which is larger (111 cm) than that of *Patagotitan* (101 cm). This femur shaft yielded an estimated body mass of 73 tons (Mazzetta et al., 2004). Two problems are found with this estimation. Firstly, as for the other femur, it cannot be referred to

Argentinosaurus and therefore the body mass of this taxon cannot be estimated using this scaling method either. Secondly, as Campione and Evans (2012) noted, scaling equations based only on femoral circumference alone have a significantly higher percent prediction error than equations based on the combined humeral and femoral circumference. Therefore, the mass estimate for this isolated femur should be taken with caution, although clearly represents an animal with larger femur circumference.

In sum, current data indicates a sauropod with a longer femoral circumference than that of *Patagotitan* existed in the Huincul Formation, but for the moment none of the femora can be confidentially referred to *Argentinosaurus huinculensis* and new remains of associated material needs tos be found in order to determine if these remains represent a taxon larger than *Patagotitan*, such as associated femoral and humeral remains (to apply the scaling equation proposed by Campione and Evans, 2012) or even more complete remains (to apply a volumetric approach proposed by Sellers et al. 2012). The *Patagotitan* materials, however, include elements (e.g., vertebrae) preserved in the type material of *Argentinosaurus* and these provide the only possible direct comparison between these two taxa (see below).

The situation for *Puertasaurus* is even more difficult, as its type material is more fragmentary than that of *Argentinosaurus*, there are neiher fragmentary remains of the femur nor the humerus, and there are no other specimens referred to this taxon. As for *Argentinosaurus*, modern quantitative approaches to body mass estimation cannot be applied for *Puertasaurus* due to the lack of sufficient material. However, as also noted by Fowler and Sullivan (2011), some elements (anterior dorsal vertebrae) are preserved in the type material of both *Argentinosaurus* and *Puertasaurus,* and also in *Patagotitan*. Comparing these elements is the only possible criterion to estimates size differences among these taxa (see below).

Vertebral area comparisons. For a size comparison between *Patagotitan* and other giant titanosaurs from Patagonia (*Argentinosaurus, Puertasaurus* and *Notocolossus*) we used the anterior dorsal vertebrae (preserved for all of them). Although interspecific allometry can bias these comparisons, the phylogenetic proximity of these taxa (figure 3) reduces the chances of extreme body plan difference among these titanosaurs. The overlapping skeletal elements between these three taxa are restricted to anterior dorsal vertebrae (D2-D3), which are the only elements preserved in all of these three titanosaur taxa.

In a similar way to the convex hull method proposed by Sellers et al. (2012) for different body segments, we created a polygon by linking each extreme point of a vertebra in anterior view (i.e., centrum, diapophyses, neural spine). This is the 2D equivalent of the minimum convex hull method used on 3D models by Sellers et al (2012). Our procedure results in a minimum polygon, for which we calculated the area (using the software ImageJ; Rasband, 2003).

In this case, we compared the second and third dorsal vertebrae of *Patagotitan* (D2 and D3) with, the recently described *Notocolossus* (D2), *Puertasaurus* (D2), and *Argentinosaurus* (D3 as interpreted by Salgado and Powell, 2010; *contra* Bonaparte and Coria, 1993) in anterior view. Three parameters were taken for vertebral comparisons depending on the preserved parts of these elements: a) the total polygon area using the entire vertebra (in anterior view), b) the dorsal polygon area (using landmarks from

parapophyses and dorsal to it), and c) total width from right to left transverse process (Fig. S6).

The total polygon area of vertebra D2 in *Patagotitan* is 1.062 m^2, which is 8.7% more than D2 of *Puertasaurus* (0.977 m^2; see Fig. S6) and 60% larger than that of *Notocolossus* (0.662m^2; see Fig. S6). The second dorsal vertebra of *Argentinosaurus* is not preserved and comparisons can only be done with D3, the validity of which is contingent on the absence of strong serial variation from D2 to D3. Furthermore, D3 of *Argentinosaurus* lacks the centrum and therefore we can only compare the dorsal polygon area (using landmarks from parapophyses and dorsal to it, such as diapophyses and neural spine; see Fig. S6). The D2 of *Patagotitan* has a dorsal polygon area of 0.703 m^2, which is 24% larger than the polygon of the D2 of *Notocolossus* (Fig. S6), 18% larger than the dorsal polygon area of D2 of *Puertasaurus*, and 12% larger than the dorsal polygon area of D3 of *Argentinosaurus* (Fig. S6). This main difference is caused because the anterior dorsal vertebrae of *Patagotitan* are both dorsoventrally higher and lateromedially wider than those of the three other giant titanosaurs (especially in the neural arch).

As we have compared so far the D2 of *Patagotitan* and the D3 of *Argentinosaurus*, and considering the expectable size variation from D2 to D3, we also compared the D3 of *Argentinosaurus* with the D3 of *Patagotitan*. Unfortunately, the neural spine of D3 in *Patagotitan* is missing, so we cannot provide the height of the neural spine or the polygon area of this element. We therefore compared the distance between the left and right diapophyses in both taxa. Whereas this distance is 127 cm in *Argentinosaurus*, in *Patagotitan* this distance is 138 cm (8% more than in *Argentinosaurus*; see Fig. S6). Using a similar approach, Fowler and Sullivan (2011) noted the width of the anterior dorsal of *Puertasaurus* was marginally smaller than that of *Argentinosaurus*. In sum, the direct comparison of the elements preserved in the three giant titanosaurs indicate that the dorsal vertebrae of *Patagotitan* are 8%–18% larger than that of *Argentinosaurus* and *Puertasaurus*, and even larger when compared to *Notocolossus*, depending on the landmarks used for comparisons. We must underscore what we stated above, we cannot extrapolate this as a relative body mass estimate for *Argentinosaurus* and *Puertasaurus* and the only way to obtain a reliable body mass estimation with currently available methods (e.g., Campione and Evans, 2012; Sellers et al., 2012) for *Argentinosaurus* and *Puertasaurus* is contingent on finding new associated material that can be referred to these taxa.

Comparisons with other skeletal measures of *Patagotitan* and other lognkosaurian sauropods are detailed below (Table S3) and indicate that, although smaller, *Quetecsaurus*, *Drusilasaura*, *Futalognkosaurus, Notocolossus,* and *Mendozasaurus* are also remarkably large titanosaurs.

Table S3. Size comparison between lognkosaurian sauropods. **Abbreviations**: **BM**, Body Mass (Campione and Evans, 2012); **CL**, Coracoid Length; **HL**, Humerus length; **DPA**, Dorsal Polygon Area; **FL**, Femur Length; **MW**, Maximum width (from left to right diapophysis); **PL**, Pubis Length; **SL**, Scapular Length; **TPA**, Total Polygon Area.

TAXA	SL (cm)	CL (cm)	HL (cm)	PL (cm)	FL (cm)	BM (kg)	TPA 2nd dorsal (m^2)	DPA 2nd-3rd dorsal (m^2)	MW 3rd dorsal (cm)
Patagotitan	196.5	61.5	167.5	140.0	238.0	69000	1.062	0.703	138.0
Drusilasaura	147.0	–	–	–	–	–	–	–	–
Futalognkosaurus	–	–	156.0	137.0	194.5	38140	?	?	?
Argentinosaurus	–	–	–	–	–	–	–	0.623	127.0
Notocolossus	–	–	176.0	–	–	–	–	–	–
Puertasaurus	–	–	–	–	–	–	0.977	0.591	–
Mendozasaurus	118.0	–	106.0	–	–	–	?	?	–
Quetecsaurus	–	32.0	–	–	–	–	–	–	–

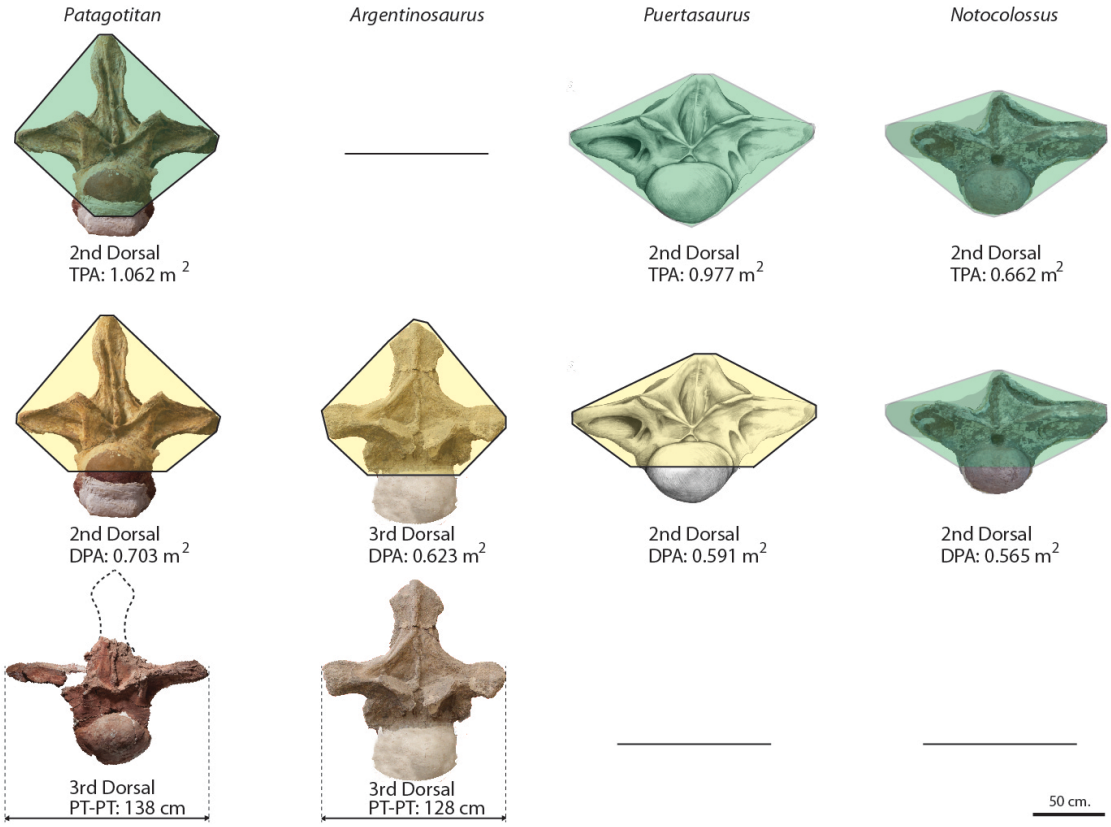

Fig. S6. Compared measurements of anterior dorsal vertebrae between *Patagotitan*, *Argentinosaurus*, *Puertasaurus,* and *Notocolossus*. **Abbreviation: DPA**: Dorsal Polygon Area (above parapophyses); **PT-PT**, horizontal distance between the extremes of the transverse processes. **TPA**, Total Polygon Area of the vertebra.

1.5. Caudal attachment for the *caudofemoralis longus* muscle. Primary and secondary lateral surfaces.

Although most caudal vertebrae of *Patagotitan* were found disarticulated from each other, the relative positions of preserved elements can be established based on their general morphology and centrum proportions, given the serial changes observed in other titanosaur sauropods (e.g., *Alamosaurus*, Gilmore, 1946; Unnamed titanosaur, Calvo et al., 1997). Based on the variation in morphology of the 23 caudal vertebrae recovered at the La Flecha quarry, and comparing the morphological variation along the caudal series of other taxa, we estimate that the total number of caudal vertebrae should be approximately 65, as in the indeterminate titanosaur from the Late Cretaceous of Neuquén province (Calvo et al., 1997).

Anteriormost caudal vertebrae of *Patagotitan* (from specimen MPEF-PV 3400) have well-developed and "wing-like" transverse processes and wide neural spines up to around caudal 10th. This morphology can be observed in the first caudal vertebra (Fig. S12), three articulated anterior caudals (3rd–5th), and two additional vertebrae identified as caudals 7th and 8th (figure 2). These centra are wider than long and a single lateral surface is present, which corresponds to the primary lateral surface *sensu* Salgado and García (2002).

More posterior preserved elements lack transverse processes, their neural spines are lateromedially thin and anteroposteriorly long, and their centrum are as long as wide or even longer than wide. These elements from a single specimen (MPEF-PV 3399) are regarded as middle to posterior caudal vertebrae, with the anteriomost having a position around caudal 15th. This interpreted position is based in other sauropods with similar caudal morphology (e.g., *Apatosaurus*; Gilmore 1936; unnamed titanosaur from Patagonia; Calvo et al., 1997).

Anterior middle caudals only have a single (primary lateral surface; figure 2), but the lateral surface of posteriormost, middle caudal vertebrae have two well-marked faces, a dorsal and a ventral one (figure 2). The dorsal of these surfaces have been named the secondary lateral surface by Salgado and García (2002), whereas the ventral one is considered homologous to the lateral surface of anteriormost caudals (the primary lateral surface *sensu* Salgado and García, 2002). Following the sequence of middle caudal vertebrae preserved in specimen MPEF-PV 3399 the primary lateral surface migrates ventrally and is progressively replaced by the secondary lateral surface.

Posterior caudal vertebrae preserved are far from being the last caudals of *Patagotitan*, both because of their size and their morphology. These caudals only have a single lateral surface (the secondary), which is transversally convex.

1.6 Phylogenetic analysis

In order to test the phylogenetic position of *Patagotitan mayorum* a cladistic analysis was performed, including the new taxon in a modified version of the data matrix published by Carballido et al. (2015). Respect to this version some modification were introduced into the data matrix, including an expanded taxon and character sampling as well as score modifications (mainly based on new information available). The complete list of modifications is described below. The resulted data matrix is composed of 87 taxa and 405 characters. The taxon sampling includes three basal sauropodomorphs, 17 basal sauropods (including *Haplocanthosaurus* which was here recovered outside Neosauropoda), 17 diplodocoids (10 rebbachisaurids, 4 dicraeosaurids, and 3 diplodocids), and 50 macronarians (22 non-titanosaur and 28 titanosaurs). From the 405 characters, 119 are from the skull region, 36 from the cervical series, 54 from the dorsal series, 4 are from ribs, 6 are for the sacral region, 53 from the caudal series, 54 for the forelimb, and 78 for the hindlimb. The data entry was made using Mesquite V 2.74 (Maddison and Maddison, 2011). From the multistate character 24 were treated as ordered (14, 61, 100, 102, 109, 115, 127, 132, 135, 136, 166, 179, 195, 256, 259, 276, 277, 278, 279, 299, 303, 346, 352, and 354).

Results

In the strict consensus tree (Fig. S7) there are four main unresolved nodes. The major one is at the base of Camarasauromorpha, and comprises some basal camarasauromorphs more derived than *Tehuelchesaurus*, brachiosaurids, and somphospondylans. This first politomy is due to the different positions in that *Lusotitan* can be placed (Fig S8) and therefore this polytomy can be completely resolved if *Lusotitan* is pruned from the MPTs (after the analysis). The second polytomy was recovered amongst brachiosaurids and is due to the different positions in that *Padillasaurus* can be placed among this clade (Fig. S8). A third polytomy was recovered at the base of Titanosauria and comprise the specifier taxon of this clade, *Andesaurus*, together with *Wintonotitan*, *Ligabuesaurus*, *Chubutisaurus* and more derived titanosaurs. The unresolved position of these taxa is due to the unstable position of *Ligabuesaurus* and *Wintonotitan* (Fig. S8). Finally the fourth large polytomy was recovered amongst lithostrotian titanosaurs more derived than *Malawisaurus* (Fig. S7). The unresolved relationship of these taxa is due to the different positions that *Nemegtosaurus* and *Trigonosaurus* can have amongst lithostrotian titanosaurs (Fig. S8). Removing these more unstable taxa from the analysis results in an almost fully resolved cladogram (Fig. S8).

Titanosauria, defined as *Andesaurus*, *Saltasaurus*, their common ancestor and all its descendants (see Systematic Definitions section) could include *Ligabuesaurus* (depending on the resolution of this taxon; Fig. S8), and is formed by the clade that includes to *Malarguesaurus*, *Ruyangosaurus* and Eutitanosauria (see Systematic Definitions section). Amongst Eutitanosauria there are two major lineages. One of these lineages is formed by eutitanosaurs more closely related to *Saltasaurus* than to *Patagotitan*. As in previous analyses (Lacovara et al., 2014), *Dreadnoughtus* plus Lithostrotia are forming this clade. The second lineage is formed by the eutitanosaurs

more closely related to *Patagotitan* than to *Salatsaurus*. This clade includes to Rinconsauria + (*Bonitasaura* + *Notocolossus* + Lognkosauria).

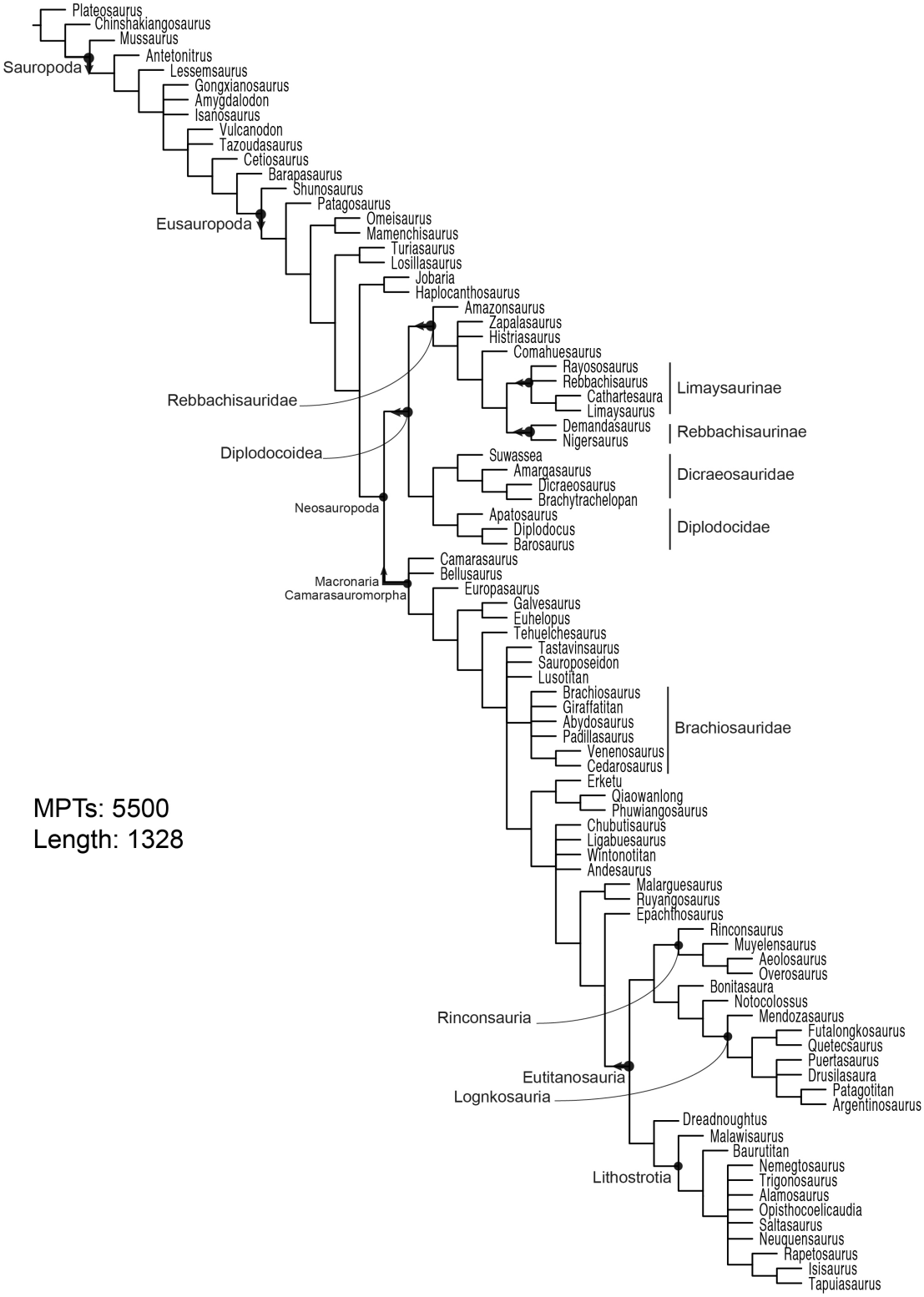

Fig. S7. Stric consesus tree obtained from the phylogenetic analysis.

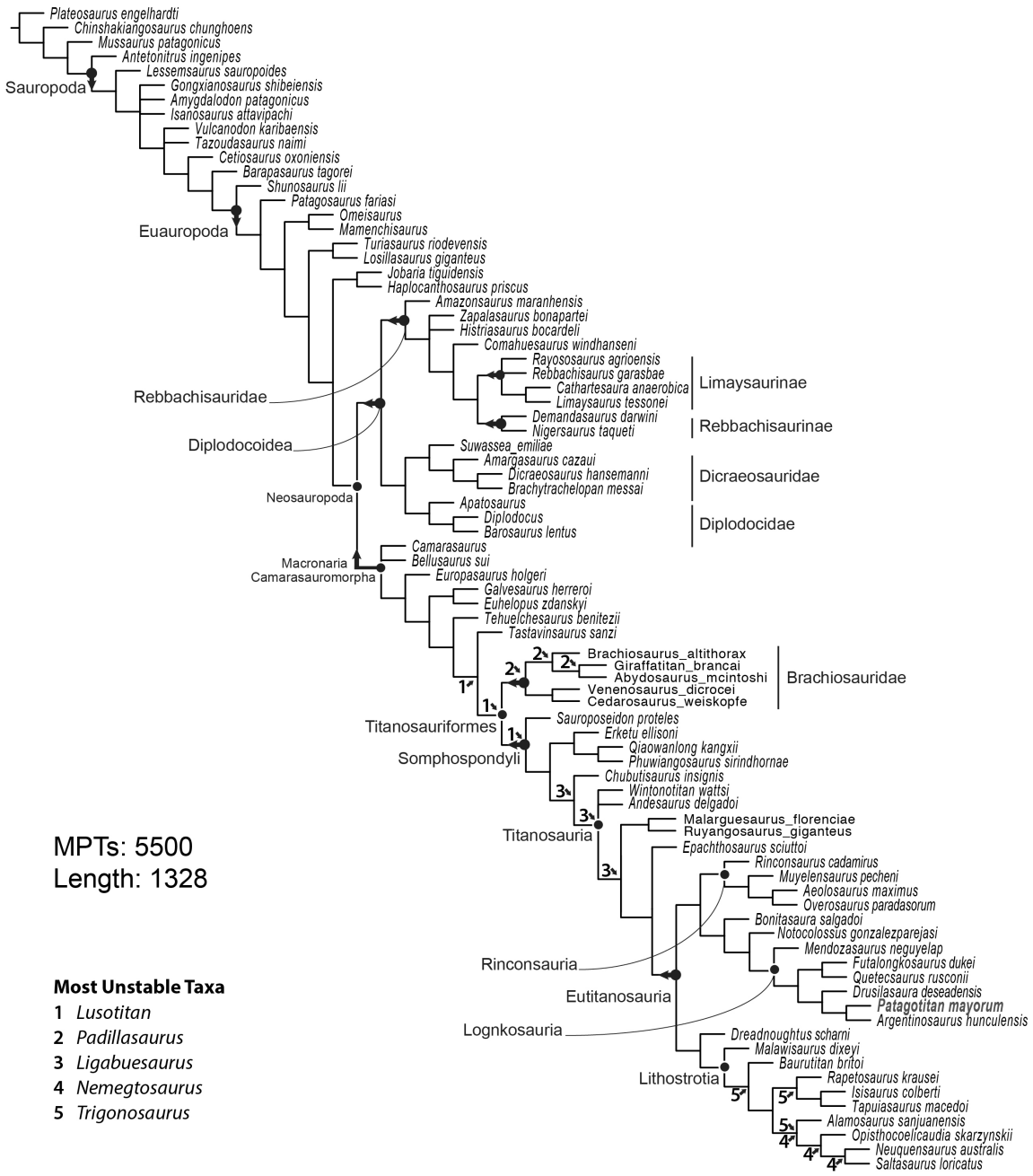

Fig. S8. Reduced consensus tree showing the possible positions of unstable taxa that caused major polytomies.

1.7 Systematic definitions followed

Titanosauria Bonaparte and Coria, 1993 (81): *Andesaurus delgadoi* Calvo and Bonaparte, 1991 (82), *Saltasaurus loricatus* Bonaparte and Powell, 1980 (83), their most recent common ancestor and all its descendants.
Comments: A complete revision of Titanosauria was discussed by Wilson and Upchurch (2003). Here we follow the node-definition made by these authors, which is based on the previously systematic definition proposed for this clade by Salgado et al. (1997).

Eutitanosauria Sanz, Powell, Le Loeuff, Martínez, and Pereda Suberbiola, 1999: All titanosaurs more closely related to *Saltasaurus loricatus* Bonaparte and Powell, 1991 than to *Epachthosaurus sciuttoi* Powell, 1990.
Comments: Eutitanosauria was initially proposed by Sanz et al. (1999) and posteriorly redefined by Salgado (2003) as a stem group of sauropods more derived than *Epachthosaurus*. This clade was mainly ignored, in part because was considered as synonymous of Saltsauridae or Saltasaurinae by Wilson and Upchurch (2003) or perhaps because was recovered as synonymous of Lithostrotia (a node defined clade formally described by Upchurch et al., 2004, but previously defined in Wilson and Upchurch, 2003). Nevertheless due to the position here recovered for *Epachthosaurus*, at the base of Titanosauria, and the more derived position of *Malawisaurus*, we considered the current definition as valid. Therefore, Eutitanosauria is currently formed by a diverse clade of derived titanosaurs composed by two unnamed main lineages, one formed by *Dreadnoughtus* + Lithostrotia and the second composed of Rinconsauria + (*Bonitasaurua* + Lognkosauria).

Rinconsauria Calvo, González Riga, and Porfiri 2007: *Muyelensaurus pecheni* Calvo, González Riga and Porfiri 2007, *Rinconsaurus caudamirus* Calvo and González Riga, 2003, their most recent common ancestor and all its descendants.

Aeolosaurini (Franco-Rosas, Salgado, Rosas, and Carvalho 2004): *Aeolosaurus rionegrinus* Powell, 1987, *Gondwanatitan faustoi* Kellner and Azevedo, 1999, their most recent common ancestor and all its descendants. (Modified here).
Comments: The original definition of Aeolosaurini was introduced by Franco-Rosas et al. (2004), but these authors did not include a phylogenetic analysis but an hypothetical phylogenetic relationships tree, in which Aeolosaurini was composed by *Aeolosaurus* and *Gondwanatitan*. A third taxon, *Rinconsaurus*, was proposed to be part of this clade as well (Franco Rosas et al., 2004:p. 332). Aeolosaurini was defined by Franco Rosas et al., (2004) as "the most inclusive clade containing *Aeolosaurus rionegrinus* and *Gondwanatitan faustoi*, but not *Saltasaurus loricatus* and *Opisthocoelicaudia skarzynskii*" (Franco Rosas et al., 2004:p. 332). This definition was subsequently followed by Santucci and Arruda-Campos (2011) whose recovered *Aeolosaurus*, *Gondwanatitan*, *Rinconsaurus*, *Panamericansaurus* and *Maxakalisaurus* as aeolosaurin titanosaurs. Based on the definition proposed by Franco Rosas et al. (2004) one of the two lineages of Eutitanosauria here recovered should be named Aeolosaurini (the one formed by Rinconsauria + (*Notocolossus* +*Bonitasauria* + Lognkosauria; Fig. S22). Nevertheless this clade is much more diverse than that proposed by Franco Rosas et al.

(2004), enclosing sauropods that were traditionally considered outside Aeolosaurini (*Notocolossus* + *Bonitasaura* + Lognkosauria). Additionally and most important, Aeolosaurini was defined and used for a branch of small derived sauropods closely related to the genus *Aeolosaurus*. In this sense it is important to note that in the majority of the phylogenetic analysis that includes *Aeolosaurus* and *Gondwanatitan*, Aeolosaurini was restricted to these two taxa and not to the monophyletic clade of titanosaurs more closely related to *Aeolosaurus* than to *Saltasaurus* (Calvo et al., 2007; González Riga et al., 2009; González Riga and Ortiz David, 2014; Salgado et al., 2015; Gallina and Otero, 2015). Therefore, and following the recommendations of the PhyloCode (Cantino and de Queiroz, 2010) the clade Aeolosaurini should be restricted to a least inclusive group of dinosaurs closely related to *Aeolosaurus*. Here we propose a new node definition for Aeolosaurini: *Aeolosaurus rionegrinus* Powell, 1987, *Gondwanatitan faustoi* Kellner and Azevedo, 1999, their most recent common ancestor and all its descendants. This definition attempts to capture the spirit of the definition and traditional use of that clade, as the PhyloCode recommends.

Lognkosauria Calvo et al. (2007) The most recent common ancestor of *Mendozasaurus neguyelap* González Riga (2005) and *Futalognkosaurus dukei* Calvo et al. (2007) and all its descendants.

Lithostrotia Upchurch et al. 2004: *Malawisaurus dixeyi* Jacobs et al. (1993), *Saltasaurus loricatus* Bonaparte and Powell, 1980, their most recent common ancestor and all its descendants.

Saltasauridae Bonaparte and Powell, 1980: The least inclusive clade containing *Opisthocoelicaudia skarzynskii* Borsuk-Bialynicka, 1977 and *Saltasaurus loricatus* Bonaparte and Powell, 1980.

Saltasaurinae Bonaparte and Powell, 1980: The most inclusive clade containing *Saltasaurus loricatus* Bonaparte and Powell, 1980 but not *Opisthocoelicaudia skarzynskii* Borsuk-Bialynicka, 1977.

1.8. Size evolution

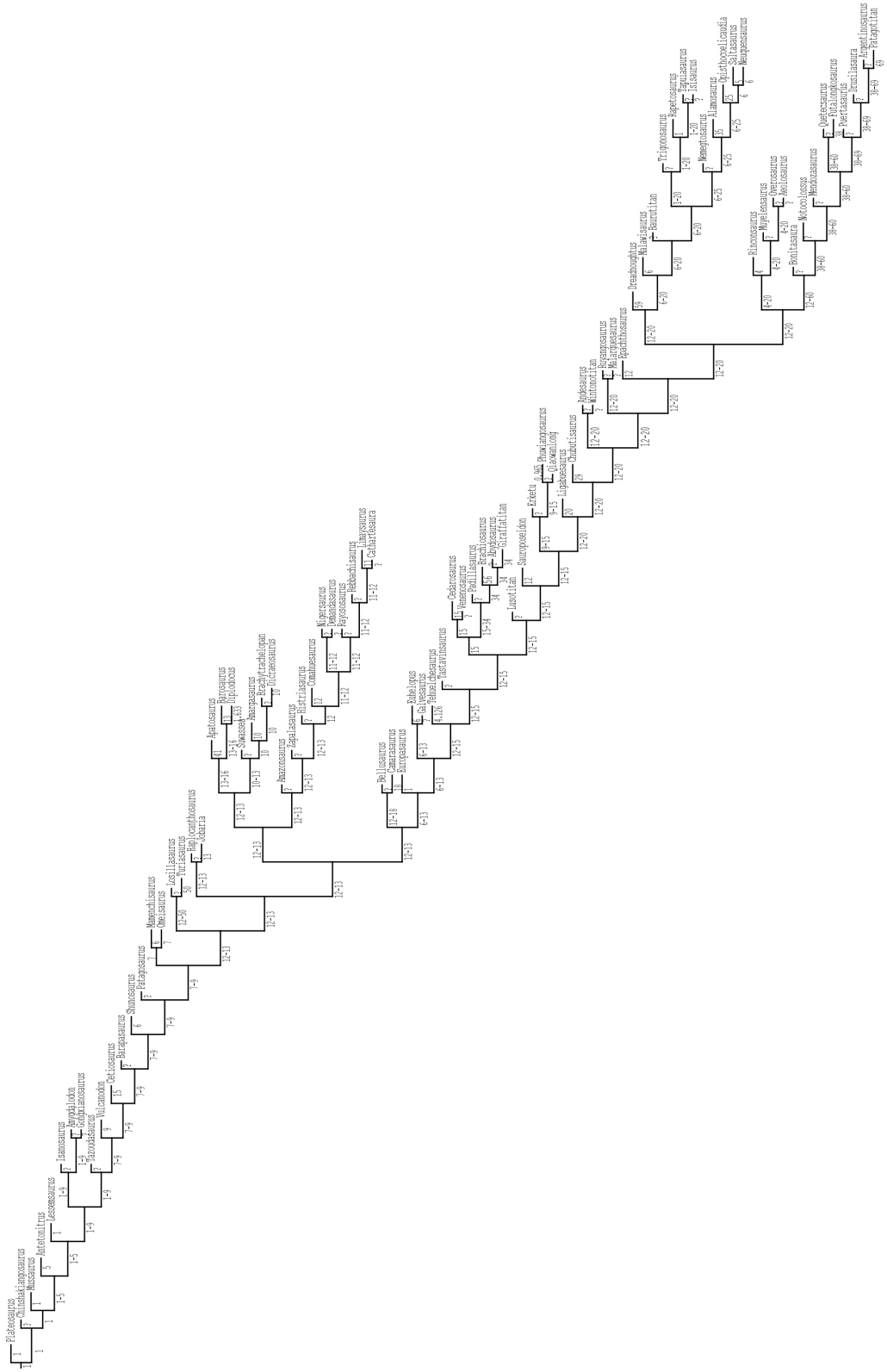

Figure S9. Body mass optimization.

1.9 Principal measurements for *Patagotitan mayorum*

Table S4. Axial Measurements. Abbreviations: /, Not preserved; **-,** Broken; ***,** Compressed; **Asp**, Assigned position; **CapL**, Centrum anteroposterior length; **CpH**, Centrum posterior height; **CpW**, Centrum posterior width.

MPEF-PV	AsP	CapL	CpW	CpH	CaPL/CpH
Cervical					
3400/1	3	47.0-	/	/	/
3400/2	5	103.5	14.5*	19.0	5.4
3400/3	7	120.0-	/	/	/
3399/1	10	74.5	17.0-*	24.0	/
3399/2	11	69.0	15.0-*	15.0*	4.6
3399/3	12	59.0	37.0	11.0*	5.3
3399/4	13	55.0	39.0	15.0*	3.6
3399/5	14	42.0	33.0	16.0*	2.6
3399/6	15	24.0*	32.0*	24.0	1.0
Dorsal					
3400/4	1	39.5*	55.0	38.0	1.0
3400/5	2	29.0*	59.0	42.5	0.6
3400/6	3	24.0*	54.0	40.0	0.6
3999/7	3	Not fully prepared yet.			
3400/7	5	31.0	42.0-	36.0-	0.8
3400/8	6	43.0-	46.5	40.0	1.0
3399/8	7	42.0*	54.0	41.5	1.0
3400/9	8	42.0	39.5-	41.0	
3399/10	8?	39.0	/	/	/
3399/09	9	39.5	41.0	40.5	0.9
3400/10	10	32.0	51.0	37.5	0.8
Caudal					
3399/11	1	36.0	36.0	46.0	0.7
3400/11	1	34.0	33.0	40.0	0.8
3400/12	3	35.0	/	44.0	0.8
3400/13	4	36.0	/	44.0	0.8
3400/14	5	35.0	29.0	36.0	0.9
3400/15	7	28.0*	37.0	40.0	0.8
3400/16	8	26.5	32	34	0.8
3399/12	19	30.0	31.0	31.0	0.9
3399/13	20	30.0	32.0	30.0	1
3399/14	21	32.0	32.5	33.0	0.9
3399/15	22	26.0	27.0	29.0	0.9

3399/16	24	28.0	24.0	27.0	1
3399/17	25	28.0	23.5	26.5	1
3399/18	26	26.0	23.0	26.0	1
3399/19	27	/	26.0	29.0	/
3399/20	28	29.0	22.0	24.0	1.2
3399/21	29	29.0	20.0	23.0	1.2
3399/22	30	27.0	28.5	21.0	1.3
3399/23	36	29.0	13.0	/	/
3399/24	37	28.0	13.5	/	/
3399/25	38	28.0	15.0	16.0	1.7
3399/26	43	27.5	16.0	16.5	1.7
3399/27	44	28.0	13.0	13.0	2.1

Table S5. Apendicular bones measurements.

Sternal Plate
(MPEF PV 3400/20)
Anteroposterior Length: 89.8
Mediolateral width: 54.5

Scapula

(MPEF PV 3400/23)
Total height: 196.5
Maximum dorsoventral height at proximal section: 111.0
Minimum dorsoventral height at mid-shaft: 40.8
Maximum dorsoventral height at distal blade: 71.5

Coracoid

(MPEF PV 3400/24)
Dorsoventral height: 114.5
Anteroposterior length: 61.5

Humerus

(MPEF-PV 3397)
Total length: 167.5
Proximal width: 62.5

Minimum width: 24.5
Distal width: 55
Circumference: 78.2

Ulna

(MPEF-PV 3399/27)
Total length: 105.0
Proximal width: 52.5
Minimum width: 23.0
Distal width: 29.0

Radius

(MPEF-PV 3399/28)
Total length: 107.0
Proximal width: 31.5
Minimum width: 19.0
Distal width: 39.0

Pubis

(MPEF-PV 3400/25)
Total length: 140.0
Proximal width: 74.0
Distal width: 57.0

Ischium

(MPEF-PV 3400/40)
Maximum length: 107.5
Proximal height: 75.5
Minimum blade height: 20.5
Maximum blade width at distal expansion: 24.0

Femur

(MPEF-PV 3400/27)
Total length: 236
Proximal width: 63.5
Minimum width: 36.0

Distal width: 68.5

(MPEF-PV 3400/27)
Total length: 235
Proximal width: 65
Minimum width: 39.0
Distal width: 67
Circumference: 93.5

(MPEF-3399/44)
Total length: 238
Proximal width: 66.0
Minimum width: 40.0
Distal width: 55 (broken)
Circunference: 101.0

1.10 Anatomical characters and changes introduced

Taxon sampling: From the 72 taxa included by Carballido et al. (2015) 16 new taxa were added, including the new species *Patagotitan mayorum*. The included taxa and source of information is provided on Table S6.

Table S6. Additional terminal taxa included in the phylogenetic analysis of Carballido et al., (2015)

Taxon	**Source of information**
Qiaowanlong You and Li, 2009	You and Li, 2009; D'Emic, 2012
Dreadnoughtus Lacovara et al., 2014	Lacovara et al., 2014
Baurutitan Kellner et al., 2005	Kellner et al., 2005
Rinconsaurus Calvo and González Riga, 2003	Pers. obs. material housed at the MRS-PV and referred to this taxon by Calvo and González Riga (2003)
Muyelensaurus Calvo et al., 2007	Pers. obs. material housed at the MRS-PV and referred to this taxon by Calvo et al. (2007)
Aeolosaurus maximus Santucci and Arruda Campos, 2011	Santucci and Arruda Campos (2011)
Overosaurus Coria et al., 2012	Pers. obs. on the holotype material (MAU-Pv-CO-439)
Ruyangosaurus Lu et al., 2009	Lu et al., 2009
Futalognkosaurus Calvo et al., 2007	Pers. obs. on the holotype specimen (MUCPv-323)
Quetecsaurus González Riga and Ortiz David, 2014	González Riga and Ortiz David (2014)
Puertasaurus Novas et al., 2005	Novas et al. (2005)
Drusilasaura Navarrete et al., 2011	Navarrete et al. (2011)
Bonitasaura Apesteguía, 2004	Apesteguía (2004); Gallina and Apesteguía (2011); Gallina and Apesteguía (2015)
Notocolossus González Riga et al., 2016	Gonzalez Riga et al. (2016)
Dreadnoughtus Lacovara et al., 2014	Lacovara et al. (2014)

Character sampling. From the 370 characters used by Carballido et al. (2015), additional character were introduced, being 23 of them taken from previous studies and 12 corresponds to new characters. Additionally 21 characters were modified in order to incorporate the new morphological information caused by the inclusion of the new taxa. The complete list of introduced and modified characters and their source is provided in Table S7.

Table S7. Introduced characters respect to the data matrix used by Carballido et al. (2015).

Character numberNº	Source	Modifications
84	Remes et al., 2009 (character number 50)	None
90	D'Emic, 2012 (character number 10)	None
101	D'Emic, 2012 (character number 15)	None
121	D'Emic, 2012 (character number 20)	None
122	D'Emic, 2012 (character number 29)	One intermediate state was added
126	Carballido et al., 2012 (character number 114)	The third state was modified
128	New	–
129	D'Emic, 2012 (character number 24)	None
130	Remes et al., 2009 (character number 79)	None
131	D'Emic, 2012 (character number 25)	Same character with different definition
146	Remes et al., 2009 (character number 78)	None
147	Salgado et al., 1997 (character number 37)	The definition was slightly changed.
148	D'Emic, 2012 (character number 28)	None
150	González Riga et al., 2009 (character number 30)	An intermediate state was added.
151	González Riga and Ortiz David, 2014 (character number 26-27)	Modification in the definition
159	Carballido et al. 2012 (character number 138)	Divided in anterior and middle
160	Carballido et al. 2012 (character number 138)	to posterior dorsals.
153	González Riga et al., 2009 (character number 32)	None
171	New	–
172	Wilson, 2002 (character number 102) Upchurch et al., 2004 (153-154)	None
173	New	–
174	New	–
175	New	–
176	New	–
185	D'Emic, 2012 (character number 49)	None
186	Pol et al., 2011 (character number 132)	None
187	Rauhut et al., 2015 (character number 46)	None
188	Rauhut et al., 2015 (character number 47)	None
189	Rauhut et al., 2015 (character number 48)	None
221	New	–
223	New	–
224	New	–
226	D'Emic, 2012 (character number 52)	None

227	D'Emic, 2012 (character number 56)	None
228	D'Emic, 2012 (character number 59)	None
242	Wilson, 2002 (character number 121)	One further state was added
243	New	–
246	New	This character was suggested as an autapomorphy of Futalognkosaurus (Calvo et al., 2007)
247	New	–
248	New	This character was suggested as an autapomorphy of *Bonitasaura* (see Gallina and Apesteguía, 2015)
253	Santucci and Arruda Campos, 2011 (character number 236)	None
254	New, based on Franco Rosas et al., 2004	–
275	New	–
276	Wilson, 2002 (character number 152)	One state was added.
291	D'Emic, 2012 (character number 76)	None
297	D'Emic, 2012 (character number 80)	None
398	D'Emic, 2012 (character number 83)	None
329	D'Emic, 2012 (character number 99)	None
347	New based in Otero, 2010	–
348	D'Emic, 2012 (character number 107)	None
349	New	–
350	New	–
351	New	–
369	D'Emic, 2012 (character number 111)	–
384	González Riga et al., 2016 (character number 331)	None
385	González Riga et al., 2016 (character number 334)	None
403	González Riga et al., 2016 (character number 348)	None
404	González Riga et al., 2016 (character number 349)	None
405	González Riga et al., 2016 (character number 350)	None

Scoring modifications. During the inclusion of the new taxa and characters added several character´s score were revised and changed on the base of new observations and publications (e.g. González Riga et al, 2016). Revised scorings of the data matrix used by Carballido et al. (2015) are here presented on Table S8. In total, 138 previous scores were modified.

Table S8. Revised scores from Carballido et al., (2015)

Taxon	Character	Modification
Amygdalodon	70	1x?
	74	1x?
Isanosaurus	278	0x1
Shunosaurus	278	0x3
Cetiosaurus	278	0x1
Patagosaurus	200	0x?
	278	0x3
Tazoudasaurus	153	1x0
Mamenchisaurus	74	?x0
Omeisaurus	197	0x1
	278	0x3
Jobaria	158	0x0/1
	278	1x0
	129	0x1
Haplocanthosaurus	278	0x3
Camarasaurus	150	0x–
Bellusaurus	278	0x3
Tehuelchesaurus	278	0x3
Europasaurus	80	?x1
	278	0x3
Tastavinsaurus	221	0x?
Euhelopus	126	2x3
	150	0x–
	278	0x3
Venenosaurus	278	0x3
Cedarosaurus	381	?x1
	382	?x1
	383	?x1
	387	?x1
	388	?x1
	394	?x1
	395	?x1
	396	?x1
	397	?x1
	398	?x1
	399	?x1
	400	?x1
	401	?x0
	402	?x0
Ligabuesaurus	108	1x2
	132	3x?
	278	0x3
	381	?x1
	382	?x1
	383	?x1

	387	?x1
	388	?x1
	389	?x1
	390	?x1
	392	?x1
Erketu	126	2x3
	133	?x0
	143	0x1
	150	0x?
Phuwiangosaurus	150	0x–
	293	1x0
	278	0x?
	342	1x0
	343	?x1
Malarguesaurus	247	0x1
Andesaurus	221	0x?
	247	?x1
	294	?x1
Epachthosaurus	184	0x1
	217	?x0
	235	?x0
	238	?x1
	239	?x0
	240	?x0
	245	?x0
	251	?x1
	253	?x1
	259	?x0
	267	?x0
	268	?x-
	269	?x1
	270	?x1
	271	?x1
	272	?x1
	273	?x1
	283	0x1
	293	?x1
	300	?x1
	302	0x1
	316	?x1
	317	?x-
	318	?x1
	319	?x1
	320	?x1
	321	?x1
	322	?x1

	323	?x1
	324	?x2
	325	?x-
	326	?x-
	335	?x0
	340	0x?
	341	1x?
	343	1x?
	358	0x1
	361	1x0
	379	?x1
	380	?x1
	402	?x0
Wintonotitan	232	0x1
	278	0x?
Mendozasaurus	124	?x1
	171	2x?
	232	2x3
	267	?x0
	283	0x1
	278	0x3
	399	?x1
	400	?x1
	401	?x1
	402	?x0
Argentinosaurus	181	0x?
	184	0x1
Malawisaurus	222	?x1
	157	1x0
Isisaurus	184	0x1
	238	1x0
	278	0x3
Rapetosaurus	281	0x?
	307	0x1
	361	1x0
Alamosaurus	19	1x?
	133	?x0
	137	0x?
	139	0x1
	140	?x0
	144	?x1
	142	0x1
	150	0x2
	155	?x3
	161	2/3x2
	169	?x1

	170	1x2
	178	2x?
	185	2x1
	194	?x1
	198	?x1
	206	0x1
	212	?x1
	216	?x1
	218	?x0
	219	?x1
	336	?x0
	283	0x1
	278	0x3
	290	1x0
	317	–x1
	381	?x1
	382	?x1
	383	?x1
	387	?x1
	388	?x1
	389	?x1
	393	?x1
	394	?x1
	396	?x1
	398	?x1
	399	?x1
	400	?x1
	402	?x0
Trigonosaurus	126	2x3
Opisthocoelicaudia	145	?x0
	152	?x1
	317	–x1
Neuquensaurus	126	2x3

Character list

Skull

(1) Posterolateral processes of premaxilla and lateral processes of maxilla, shape: without midline contact (0); with midline contact forming marked narial depression, subnarial foramen not visible laterally (1). (Wilson, 2002:character number 1).

(2) Premaxillary anterior margin shape: without step (0); with marked step but short step (1); with marked and long step (2) (modified from Wilson, 2002:character number 2).

(3) Premaxila, ascending process shape in lateral view: convex (0); concave, with a large dorsal projection (1); sub-rectilinear and directed posterodorsally (2). (Whitlock, 2011:character number 3)

(4) Premaxilla, external surface: without anteroventrally orientated vascular grooves originating from an opening in the maxillary contact (0); vascular grooves present (1). (Whitlock, 2011:character number 2)

(5) Premaxilla-maxilla suture, shape: planar (0); twisted along its length, giving the contact a sinuous appearance in lateral view (1). (D'Emic, 2012:character number 2)

(6) Premaxilla, small finger-like, vertically oriented premaxillary process near anteromedial corner of external naris: (0) absent; (1) present. (D'Emic, 2012:character number 3)

(7) Maxillary border of external naris, length: short, making up much less than one-fourth narial perimeter (0); long, making up more than one third narial perimeter (1). (Wilson, 2002:character number 3).

(8) Maxilla, foramen anterior to the preantorbital fenestra : absent (0); present (1). (Zaher *et al.*, 2011:character number 244).

(9) Preanteorbital fenestra: absent (0); present, being wide and laterally opened (1). (Modified from Wilson, 2002:character number 4).

(10) Subnarial foramen and exterior maxillary foramen, position: well distanced from one another (0); separated by narrow bony isthmus (1). (Wilson, 2002:character number 5)

(11) Antorobital fenestra: much shorter than orbital maximum diameter, less than 85% of orbit (0); subequal to orbital maximum diameter, greater than 85% orbit (1). (Modified from Wilson, 2002:character number 6 following to Whitlock, 2011:character number 13)

(12) Antorbital fenestra, shape of dorsal margin: straight or convex (0); concave (1). (Whitlock, 2011:character number 14).

(13) Antorbital fossa: present (0); absent (1). (Wilson, 2002:character number 7)

(14) External nares position: terminal (0); retracted to level of orbit (1); retracted to a position between orbits (2). (Wilson, 2002:character number 8)

(15) External nares, maximum diameter: shorter (0); or longer than orbital maximum diameter (1). (Wilson, 2002:character number 9)

(16) Orbital ventral margin, anteroposterior length: broad, with subcircular orbital margin (0); reduced, with acute orbital margin (1). (Wilson, 2002:character number 10)

(17) Lacrimal, anterior process: present (0); absent (1). (Wilson, 2002:character number 11)

(18) Lacrimal, anteriorly projecting vertical plate of bone: absent (0); present (1). (D'Emic, 2012: character number 4)

(19) Jugal contribution to the ventral border of the skull: present and long (0); absent or very reduced (1). (Carballido et al., 2012:character number 16).

(20) Quadratojugal-Maxilla contact: absent or small (0); broad (1). (Whitlock, 2011:character number 10).

(21) Jugal-ectopterygoid contact: present (0); absent (1). (Wilson, 2002:character number 12)

(22) Jugal, contribution to antorbital fenestra: absent (0); present, but very reduced (1); present and large, bordering approximately one-third its perimeter (2). (Modified from Wilson, 2002:character number 13).

(23) Quadratojugal, position of anterior terminus: posterior to middle of orbit (0); anterior margin of orbit or beyond (1). (Whitlock, 2011:character number 30).

(24) Quadratojugal, anterior process length: short, anterior process shorter than dorsal process (0); long, anterior process more than twice as long as dorsal process (1). (Wilson, 2002:character number 32)

(25) Quadratojugal, angle between anterior and dorsal processes: less than or equal to 90°, so that the quadrate shaft is directed dorsally (0); greater than 90°, approaching 130°, so that the quadrate shaft slants posterodorsally (1). Whitlock, 2011:character number 31).

(26) Ventral edge of anterior surface of the quadratojugal: straight, not expanded ventrally (0); Slightly expanded ventrally, forming a small bulge, which height is less than twice the ramus height (1); well expanded ventrally, forming a notorious bulge, which height is twice or more the minimum height of the ramus (2). (Modified from Upchurch et al., 2004:character number 26)

(27) Squamosal contribution to the supratemporal fenestra: present, the squamosal is well visible in dorsal view (0); reduced or absent (1). (Curry Rogers, 2005:character number 37).

(28) Squamosal-quadratojugal contact: present (0); absent (1). (Wilson, 2002:character number 31)

(29) Squamosal, posteroventral margin: smooth (0); "with prominent, ventrally directed ""prong"" (1). (Whitlock, 2011:character number 37).

(30) Prefrontal posterior process size: small, not projecting far posterior of frontal-nasal suture (0); elongate, approaching parietal (1). (Wilson, 2002:character number 14)

(31) Prefrontal, posterior process shape: flat (0); hooked (1). (Wilson, 2002:character number 15)

(32) Prefrontal, anterior process: absent (0); present (1). (Curry Rogers, 2005:character number 30)

(33) Prefrontal-Frontal contact width: large, equal or longer that the anteroposterior length of the prefrontal (0); narrow, less than half the anteroposterior length of the prefrontal (1). (Zaher *et al.*, 2011:character number 239).

(34) Postorbital, ventral process shape: transversely narrow (0); broader transversely than anteroposteriorly (1). (Wilson, 2002:character number 16).

(35) Postorbital, posterior process: present (0); absent (1). (Wilson, 2002:character number 17).

(36) Postorbital, posterior margin articulating with the squamosal : with tapering posterior process (0); with a deep posterior process (1). (Zaher *et al.*, 2011:character number 245).

(37) Frontal contribution to supratemporal fossa: present (0); absent (1). (Wilson, 2002:character number 18)

(38) Frontals, midline contact (symphysis): sutured (0); or fused in adult individuals (1). (Wilson, 2002:character number 19)

(39) Frontal, anteroposterior length: approximately twice (0); or less than minimum transverse breadth (1). (Wilson, 2002:character number 20)

(40) Frontal-nasal suture, shape: flat or slightly bowed anteriorly (0); V-shaped, pointing posteriorly (1). (Whitlock, 2011:character number 21)

(41) Frontals, dorsal surface: without paired grooves facing anterodorsally (0); grooves present, extend on to nasal (1). (Whitlock, 2011:character number 22)

(42) Frontal, contribution to dorsal margin of orbit: contribution to dorsal margin of orbit: less than 1.5 times the contribution of prefrontal (0); at least 1.5 times the contribution of prefrontal (1). (Whitlock, 2011:character number 23)

(43) Parietal occipital process, dorsoventral height: short, less than the diameter of the foramen magnum (0); deep, nearly twice the diameter of the foramen magnum (1). (Wilson, 2002:character number21)

(44) Parietal, contribution to post-temporal fenestra: present (0); absent (1). (Wilson, 2002:character number 22)

(45) Parietal, distance separating supratemporal fenestrae: less than the long axis of supratemporal fenestra, 0.8 or less (0); almost the same than the long axis of supratemporal fenestra 0.8-1.2 (1); much larger than the long axis of supratemporal fenestra more than 1.2 (2). (Modified from Wilson, 2002: character number 24).

(46) Postparietal foramen: absent (0); present (1). (Wilson, 2002:character number 23)

(47) Paroccipital process distal terminus:: straight, slightly expanded surface (0); rounded, tongue-like process (1). (Whitlock, 2011:character number 42)

(48) Supratemporal fenestra: present (0); absent (1). (Wilson, 2002:character number 25)

(49) Supratemporal fenestra, long axis orientation: anteroposterior (0); transverse (1). (Wilson, 2002:character number26)

(50) Supratemporal fenestra, maximum diameter: much longer than (0); or subequal to that of foramen magnum (1). (Wilson, 2002:character number 27)

(51) Supratemporal region, anteroposterior length: temporal bar longer (0); or shorter anteroposteriorly than transversely (1). (Wilson, 2002:character number 28)

(52) Supratemporal fossa, lateral exposure: not visible laterally, obscured by temporal bar (0); visible laterally, temporal bar shifted ventrally (1). (Wilson, 2002:character number 29)

(53) Supraoccipital, sagital nuchal crest: broad, weakly developed (0); narrow, sharp and distinct (1). (Whitlock, 2011:character number 45).

(54) Laterotemporal fenestra, anterior extension: posterior to orbit (0); ventral to orbit (1). (Wilson, 2002:character number 30)
(55) Quadrate fossa: absent (0); present (1). (Wilson, 2002:character number 33)
(56) Quadrate fossa, depth: shallow (0); deeply invaginated (1). (Wilson, 2002:character number 34)
(57) Quadrate fossa, orientation: posterior (0); posterolateral (1). (Wilson, 2002:character number 35)
(58) Quadrate, articular surface shape: quadrangular in ventral view, oriented transversely (0); roughly triangular in shape or thin, crescent-shaped surface with anteriorly directed medial process (1). (Modified *sensu* Mannion *et al.,* 2011. from Whitlock, 2011:character number 32).
(59) Quadrate, articular surface shape: quadrangular in ventral view, oriented transversely or roughly triangular in shape (0); thin, crescent-shaped surface with anteriorly directed medial process (1). (Modified sensu Mannion *et al.,* 2011 from Whitlock, 2011:character number 32).
(60) Palatobasal contact, shape: pterygoid with small facet (0); dorsomedially orientated hook (1); or rocker-like surface for basipterygoid articulation (2). (Wilson, 2002:character number 36)
(61) Pterygoid, transverse flange (i.e. ectopterygoid process) position: posterior of orbit (0); between orbit and antorbital fenestra (1); anterior to antorbital fenestra (2). (Wilson, 2002:character number37)
(62) Pterygoid, quadrate flange size: large, palatobasal and quadrate articulations well separated (0); small, palatobasal and quadrate articulations approach (1). (Wilson, 2002:character number 38)
(63) Pterygoid, palatine ramus shape: straight, at level of dorsal margin of quadrate ramus (0); stepped, raised above level of quadrate ramus (1). (Wilson, 2002:character number39)
(64) Pterygoid, sutural contact with ectopterygoid: broad, along the medial or lateral surface (0); narrow, restricted to the anterior tip of the ectopterygoid (1). (Zaher et al. 2011:character number 240)
(65) Palatine, lateral ramus shape: plate-shaped (long maxillary contact) (0); rod-shaped (narrow maxillary contact) (1). (Wilson, 2002:character number 40)
(66) Epipterygoid: present (0); absent (1). (Wilson, 2002:character number 41)
(67) Vomer, anterior articulation: maxilla (0); premaxilla (1). (Wilson, 2002:character number 42)
(68) Supraoccipital, height: twice subequal to (0); or less than height of foramen magnum (1). (Wilson, 2002:character number 43)
(69) Paroccipital process, ventral non-articular process: absent (0); present (1). (Wilson, 2002:character number 44)
(70) Crista prootica, size: rudimentary (0); expanded laterally into dorsolateral process (1). (Wilson, 2002:character number 45)
(71) Basipterygoid processes, length: short, approximately twice (0); or elongate, at least four times basal diameter (1). (Wilson, 2002:character number 46)
(72) Basipterygoid processes, angle of divergence: approximately 45° (0); less than 30° (1). (Wilson, 2002:character number 47)

(73) Basal tubera, anteroposterior depth: approximately half dorsoventral height (0); sheet-like, 20% dorsoventral height (1). (Wilson, 2002:character number 48)

(74) Basal tubera, breadth: much broader than (0); or narrower than occipital condyle (1). (Wilson, 2002:character number 49)

(75) Basal tubera: distinct from basipterygoid (0); reduced to slight swelling on ventral surface of basipterygoid (1). (Whitlock, 2011:character number 53)

(76) Basal tubera, shape of posterior face: convex (0); slightly concave (1). (Whitlock, 2011:character number 54)

(77) Basioccipital depression between foramen magnum and basal tubera: absent (0); present (1). (Wilson, 2002:character number 50)

(78) Basisphenoid/basipterygoid recess: present (0); absent (1). (Wilson, 2002:character number 51)

(79) Basisphenoid/quadrate contact: absent (0); present (1). (Wilson, 2002)

(80) Basisphenoid, sagital ridge between basipterygoid processes: absent (0); present (1). (Zaher *et al.*, 2011:character number 242)

(81) Basipterygoid processes, orientation: perpendicular to (0); or angled approximately 45° to skull roof (1). (Wilson, 2002:character number 53)

(82) Basipterygoid, area between the basipterygoid processes and parasphenoid rostrum: is a mildly concave subtriangular region (0); forms a deep slot-like cavity that passes posteriorly between the bases of the basipterygoid processes (1). (Mannion *et al.*, 2013:character number 48)

(83) Occipital region of skull, shape: anteroposteriorly deep, paroccipital processes oriented posterolaterally (0); flat, paroccipital processes oriented transversely (1). (Wilson, 2002:character number 54)

(84) Occipital condyle, lateral surface of the basioccipital: flat or slightly convex (0); strongly concave (1). (Remes et al., 2009:character number 50)

(85) Dentary, depth of anterior end of ramus: slightly less than that of dentary at mid-length (0); 150% minimum depth (1). (Wilson, 2002:character number 55)

(86) Dentary, anteroventral margin shape: gently rounded (0); sharply projecting triangular process (1). (Wilson, 2002:character number 56)

(87) Dentary symphysis, orientation: angled 15° or more anteriorly to (0); or perpendicular to axis of jaw ramus (1). (Wilson, 2002:character number 57)

(88) Dentary, cross-sectional shape of symphysis: oblong or rectangular (0); subtriangular, tapering sharply towards ventral extreme (1); subcircular (2). (Whitlock, 2011:character number 60)

(89) Dentary, tuberocity on labial surface near symphysis: absent (0); present (1). (Whitlock, 2011:character number 57)

(90) Dentary, posteroventral process shape: single (0); divided (1). (D'Emic, 2012:character number 10)

(91) Mandible, coronoid eminence: strongly expressed, clearly rising above plane of dentigerous portion (0); absent (1). (Whitlock, 2011:character number 62)

(92) External mandibular fenestra: present (0); absent (1). (Wilson, 2002:character number 58)

(93) Surangular depth: less than twice (0); or more than two and one-half times maximum depth of the angular (1). (Wilson, 2002:character number 59)

(94) Surangular ridge separating adductor and articular fossae: absent (0); present (1). (Wilson, 2002:character number 60)

(95) Adductor fossa, medial wall depth: shallow (0); deep, prearticular expanded dorsoventrally (1). (Wilson, 2002:character number 61)

(96) Splenial posterior process, position: overlapping angular (0); separating anterior portions of prearticular and angular (1). (Wilson, 2002:character number 62)

(97) Splenial posterodorsal process: present, approaching margin of adductor chamber (0); absent (1). (Wilson, 2002:character number 63)

(98) Coronoid, size: extending to dorsal margin of jaw (0); reduced, not extending dorsal to splenial (1); absent (2). (Wilson, 2002:character number 64)

(99) Tooth rows, shape of anterior portions: narrowly arched, anterior portion of tooth rows V-shaped (0); broadly arched, anterior portion of tooth rows U-shaped (1); rectangular, tooth-bearing portion of jaw perpendicular to jaw rami (2). (Wilson, 2002:character number 65)

(100) Tooth rows, length: extending to orbit (0); restricted anterior to orbit (1); restricted anterior to antorbital fenestra (2); restricted anterior to subnarial foramen (3). (Modified from Wilson, 2002:character number 66)

(101) Maxillary teeth shape: straight along axis (0); twisted axially through an arc of 30-45º: absent (0); present (1). (D'Emic, 2012:character number 15)

(102) Dentary teeth, number: greater than 20 (0); 10-17 (1); 9 or fewer (2). (Modified from Wilson, 2002:character number73)

(103) Replacement teeth per alveolus, number: two or fewer (0); more than four (1). (Wilson, 2002:character number 74)

(104) Lateral plate: absent (0); present (1). (Upchurch et al., 2004:character number 9)

(105) Teeth, orientation: perpendicular (0); or oriented anteriorly relative to jaw margin (1). (Wilson, 2002:character number 75)

(106) Tooth crowns, orientation: aligned along jaw axis, crowns do not overlap (0); aligned slightly anterolingually, tooth crowns overlap (1). (Wilson, 2002:character number 69)

(107) Tooth crowns, shape: narrow crowns (0); broad crowns (1).

(108) Tooth crowns, cross-sectional shape at mid-crown: elliptical (0); D-shaped (1); sub-cylindrical (2); cylindrical (3). (Wilson, 2002:character number 70)

(109) SI values for tooth crowns: less than 3.0 (0); 3.0-4.0 (1); 4.0-5.0 (2); more than 5.0 (3). (Upchurch *et al.*, 2004:chs. 67-69)

(110) Crown-to-crown occlusion: absent (0); present (1). (Wilson, 2002:character number 67)

(111) V-shaped wear facets: present (0); absent (1). (Modified from Wilson, 2002:character number 68)

(112) Development of the marginal wear facets: well developed (0); slightly developed as marginal facets (1).

(113) One high angle wear facet and a second low angle wear facet: absent (0); present (1).

(114) Single planar wear facet in labial or lingual surface of the teeth: absent (0); present (1).

(115) Marginal tooth denticles: present (0); absent on posterior edge (1); absent on both anterior and posterior edges (2). (Wilson, 2002:character number 72)

(116) Enamel surface texture: smooth (0); wrinkled (1). (Wilson, 2002:character number71)

(117) Thickness of enamel asymmetric labiolingually: absent (0); present (1). (Whitlock, 2011:character number 74)

(118) Teeth, longitudinal grooves on lingual aspect: absent (0); present (1). (Wilson, 2002:character number 76)

Cervical vertebrae

(119) Cervical vertebrae, number: 10 or fewer (0); 12 (1); 13-14 (2); 15 (3); 16 or more (4). (Modified from Wilson, 2002:character number 80 and Upchurch *et al.*, 2004:chs. 96-100)

(120) Atlas, intercentrum occipital facet shape: rectangular in lateral view, length of dorsal aspect subequal to that of ventral aspect (0); expanded anteroventrally in lateral view, anteroposterior length of dorsal aspect shorter tan that of ventral aspect (1). (Wilson, 2002:character number 79)

(121) Axis, centrum shape: over two and a half times as long as tall (0); less than twice as long as tall (1). (D'Emic, 2012: character number 20)

(122) Cervical vertebrae, parapophyses, shape and orientation: short and weakly developed, projected laterally or slightly ventrally (0); middle development, ventrally such that the cervical ribs are displaced ventrally around half the height of the centrum (1); well developed, broad and ventrally projected such that cervical ribs are displaced ventrally more than the height of the centrum (2). (Modified from D'Emic, 2012:character number 29)

(123) Cervical centra, articulations: amphicoelous (0); opisthocoelous (1). (Salgado *et al.*, 1997:character number 1 ; Wilson, 2002:character number 82; Upchurch, 1998:character number 81 and Upchurch *et al.*, 2004:character number 103)

(124) Cervical centra, ventral surface: is flat or slightly convex transversely (0); transversely concave (1). (Upchurch, 1998:character number 84 and Upchurch *et al.*, 2004:character number 107)

(125) Cervical centra, midline keels on ventral surface: prominent and plate-like (0); reduced to low ridges or absent (1). (Upchurch, 1998:character number 83 and Upchurch *et al.*, 2004:character number 106)

(126) Cervical centra, pleurocoels: absent (0); present with well defined anterior, dorsal, and ventral edges, but not the posterior one (1); present, with well defined edges (2); absent, but with deep lateral fossa which bears small pneumatopores that communicate to the interior pneumatic cavities. (3).

(127) Cervical centra, pleurocoels: singles without division (0); with a well defined anterior excavation and a posterior smooth fossa (1); divided by a bone septum, resulting in an anterior and a posterior lateral excavation (2); divided in three or more lateral excavations, resulting in a complex morphology (3); with a well defined anterior excavation and a posterior smooth fossa (Modified from Salgado *et al.*, 1997; Wilson, 2002; Harris, 2006)

(128) Cervical vertebrae, well developed epipophyses: absent (0); present (1).

(129) Cervical vertebrae, epipophyses shape: stout, pillar like expansions above postzygapophyses (0); posteriorly projecting prongs (1). (D'Emic, 2012:character number 24)

(130) Prezygapophyses, anterior process suited ventrolaterally to the articular surface: absent (0); present (1). (Remes et al., 2009:character number 79)

(131) Cervical vertebrae with an accessory lamina, which runs from the PODL (or slightly anteriorly) up to the SPOL: absent (0); present (1). (Modified from D'Emic, 2012:character number 25)

(132) Cervical vertebrae, height divided width (measured in its posterior articular surface): higher than 1.1 (0), around 1 (1); between 0.9 and 0.7 (2); smaller than 0.7 (3). (Modified from Wilson, 2002:character number 84; Upchurch,1998:character number 85 and Upchurch *et al.*, 2004:character number 108)

(133) Cervical centra, small notch in the dorsal margin of the posterior articular surface: absent (0); present (1). (Carballido et al., 2012)

(134) Cervical vertebrae, neural arch lamination: well developed, with well marked laminae and fossae (0); rudimentary, with diapophyseal laminae absents or very slightly marked (1). (Wilson, 2002:ch, 81)

(135) Cervical vertebrae with an accessory lamina, which runs from the postzygodiapophyseal lamina (PODL) up to the spinoprezygapophyseal lamina (SPRL): absent (0); present (1). (Modified from Sereno *et al.*, 2007:chs. 50, 51; Whitlock, 2011:chs. 78, 96).

(136) Cervical centra, internal pneumaticity: absent (0); present with singles and wide cavities (1); present, with several small and complex internal cavities (2). (Modified from Carballido et al., 2011)

(137) Anterior cervical vertebrae, prespinal lamina: absent (0); present (1). (Carballido et al., 2012).

(138) Anterior cervical vertebrae, neural spine shape: single (0); bifid (1). (Wilson, 2002:character number 72; Upchurch *et al.*, 2004:character number 118)

(139) Middle and posterior cervical vertebrae, prespinal lamina: absent (0); present (1). (Carballido et al., 2012).

(140) Middle cervical vertebrae, lateral fossae on the prezygapophysis process: absent (0); present (1). (Harris, 2006).

(141) Middle, cervical vertebrae, height of the neural arch: less than the height of the posterior articular surface (0); higher than the height of the posterior articular surface (1). (Wilson, 2002:character number 87; similar Upchurch *et al.*, 2004:111 and 112)

(142) Middle cervical centrum, anteroposterior length divided the height of the posterior articular surface: less than 4 (0); more than 4 (1). (Wilson, 2002:character number 74; and Upchurch *et al.*, 2004:character number 102).

(143) Middle and posterior cervical vertebrae, morphology of the centroprezygapophyseal lamina: single (0); dorsally divided, resulting in a lateral and medial lamina, being the medial lamina linked with the intraprezygapophyseal lamina and not with the prezygapophysis (1); divided, resulting in the presence of a "true" divided centroprezygapophyseal lamina, which is dorsally connected to the prezygapophisis (2). (Carballido et al., 2012).

(144) Middle and posterior cervical vertebrae, morphology of the centropostzygapophyseal lamina (CPOL): single (0); divided, with the medial part contacting the intrapostzygapophyseal lamina (1) (Carballido et al., 2012)

(145) Middle and posterior cervical vertebrae, articular surface of zygapophyses: flat (0); transversally convex (1). (Upchurch *et al.,* 2004)

(146) Middle and posterior cervical vertebrae, prominent triangular flange on posterior edge of the diapophyseal process (in the PCDL): absent (0); present (1). (Remes et al., 2009: character number 78)

(147) Middle cervical vertebrae, prezygapophyses position: do not extend beyond the anterior margin of the centrum (0); extends beyond the anterior margin of the centrum (1). (Salgado et al., 1997:ch 37)

(148) Middle and posterior cervical vertebrae, parapophysis shape: subcircular (0); anteroposteriorly elongate (1). (D'Emic, 2012:character number 28)

(149) Posterior cervical vertebrae, lateral profile of the neural spine: displays steeply sloping cranial and caudal faces (0); displays steeply sloping cranial face and noticeably less steep caudal margin (1). (Upchurch *et al.*, 2004:character number 119)

(150) Posterior cervical vertebrae, neural spine shape: not expanded distally (0); expanded but not as much as the width of the centrum (1); laterally expanded, being equal or wider than the vertebral centrum (1). (Modified from González Riga *et al.*, 2009)

(151) Posterior cervical vertebrae, lateral expansion: SPRLs does not contact the lateral margins of the neural spine (0); SPRLs are contacting the lateral margins of the neural spine (1). (Modified from González Riga and Ortiz, 2014: character number 26-27)

(152) Posterior cervical and anterior dorsal vertebrae, neural spine shape: single (0); bifid (1). (Wilson, 2002:character number 90, Upchurch *et al.*, 2004:character number 118)

(153) Posterior cervical vertebrae, proportions – ratio total height / centrum length: less than 1.5 (0); more than 1.5 (1). (González Riga et al., 2009 (character number 32)

(154) Posterior cervical and anterior dorsal bifid neural spines, median tubercle: absent (0); present (1).

Dorsal vertebrae

(155) Number of dorsal vertebrae: 14 or more (0); 13 (1); 12 (2); 10 (3). (Modified from Wilson, 2002:character number 91; Upchurch *et al.* 2004:character number 122-125)

(156) Dorsal centra, pleurocoels: absent (0); present (1). (Wilson, 2002:character number 78; Upchurch *et al.* 2004:128)

(157) Dorsal vertebrae, transverse processes: are directed laterally or slightly upwards (0); are directed strongly dorsolaterally (1). (Upchurch *et al.*, 2004:character number 138)

(158) Dorsal vertebrae, distal end of the transverse process: curves smoothly into the dorsal surface of the process (0); is set off from the dorsal surface, the latter having a distinct dorsally facing flattened area (1). (Upchurch *et al.*, 2004:character number 140)

(159) Anterior dorsal vertebrae, non bifid neural spine in anterior or posterior view: posses subparallel lateral margins (0); posses lateral margins which slightly diverge dorsally (1); posses lateral margins which strongly diverge dorsally (2). (Modified

from Wilson, 2002:character number 107; Upchurch *et al.*, 2004:character number 155)

(160) Middle to posterior dorsal vertebrae, non bifid neural spine in anterior or posterior view: posses subparallel lateral margins (0); posses lateral margins which slightly diverge dorsally (1); posses lateral margins which strongly diverge dorsally (2). (Modified from Wilson, 2002:character number 107; Upchurch *et al.*, 2004:character number 155)

(161) Dorsal centra, pneumatic structures: absent, dorsal centra with solid internal structure (0); present, dorsal centra with simple and big air-spaces (camerate) (1); present, dorsal centra with small and complex air-spaces (polycamerate) (2); present, dorsal centra with small and complex air spaces (semicamellate/camellate) (3). (Modified from Carballido et al., 2011)

(162) Anterior and middle dorsal neural spines, spinoprezygapophyseal lamina (SPRL): absent (0); present (1). (Modified from Upchurch *et al.* (2007:character number 131).

(163) Posterior dorsal neural spines, spinoprezygapophyseal lamina (SPRL): absent (0); present (1). (Modified from Upchurch *et al.*, 2007:character number 132).

(164) Dorsal vertebrae, single not bifid neural spines, single prespinal lamina (PRSL): absent (0); present (1). (Modified from Salgado *et al.*, 1997:character number14)

(165) Dorsal vertebrae, single not bifid neural spines, single prespinal lamina (PRSL): rough and wide, present in the dorsalmost part of the neural spine (0); rough and wide, extended trough almost all the neural spine (1); smooth and narrow (2). (Carballido et al., 2012)

(166) Dorsal vertebrae with single neural spines, middle single fossa projected through the middline of the neural spine: present (0); absent (1). (Carballido et al., 2012)

(167) Dorsal vertebrae with single neural spines, middle single fossa, projected through the midline of the neural spine: relatively wide median simple fossa (0); a thin median simple fossa (1); extremely reduced median simple fossa (2). (Carballido et al., 2012)

(168) Anterior dorsal centra, articular face shape: amphicoelous (0); opisthocoelous (1). (Wilson, 2002:character number 94; Upchurch *et al.*, 2004:character number 104)

(169) Anterior and middle dorsal centra, pleurocoels: have rounded caudal margins (0); have tapering, acute caudal margins (1). (Salgado *et al.*, 1997; Upchurch, 1998:character number 06; Upchurch *et al.*, 2004:ca 127)

(170) Middle dorsal neural arches in lateral view, anterior edge of the neural spine: project anteriorly to the diapophysis (0); converge with the diapophysis (1); project posteriorly to the diapophysis (2). (Carballido et al., 2012)

(171) Anterior and middle dorsal vertebrae, zygapophyseal articulation angle: horizontal or slightly posteroventrally oriented (0); posteroventraly oriented (around 30º) (1); strongly posteroventraly oriented (more than 40º) (2). (Carballido et al., in 2012)

(172) Anterior dorsal vertebrae, neural spine orientation: vertical, or slightly inclined (less than 20º) (0); posterodorsally, more than 20º (1); anteriorly directed (2).

(173) Anterior dorsal vertebrae neural spine, triangular aliform processes: absent (0); present but do not project far laterally (not as far as caudal zygapophyses) (1); present and project far laterally (as far as caudal zygapophyses) (2). (Modified from Wilson, 2002:character number 102 and Upchurch *et al.*, 2004:chs. 153-154).

(174) Anterior dorsal vertebrae, neural spine minimums width / length: 0.5 or greater (stout and short neural spine) (0); lower than 0.5 (thin and tall neural spines).

(175) Anterior dorsal vertebrae, neural spine length (from TPRL to top): less than the height of the centrum (0); slightly higher than the centrum (1); twice or more the height of the centrum (2).

(176) Anterior dorsal vertebrae, dorsal edge of the neural spine: flat (0); arrow shaped (1); convex (2).

(177) Posterior dorsal vertebrae, dorsal edge of the neural spine: flat (0); arrow shaped (1); convex (2).

(178) Middle to posterior dorsal centra, ventral surface: convex transversely (0); flattened (1); is slightly concave, sometimes with one or two crests (2). (Upchurch *et al.*, 2004)

(179) Middle dorsal vertebrae, hyposphene-hypantrum system: present (0); absent (1). (Modified from Salgado *et al.*, 1997:character number 25; Wilson, 2002:character number 106; Upchurch *et al.,* 2004:character number 145)

(180) Posterior dorsal vertebrae, hyposphene-hypantrum system: present and well developed, usually with a rhomboid shape (0); present and weakly developed, mainly as a laminar articulation (1); absent or only present in posteriormost dorsal vertebrae (2). (Carballido et al., 2012)

(181) Middle and posterior dorsal vertebrae, transverse processes length: short (0); long (projecting along 1.5 the articular surface width) (1). (Carballido et al., 2012)

(182) Mid and posterior dorsal vertebrae with a single lamina (the single TPOL) supporting the hyposphene or postzygapophysis from below: absent (0); present (1). (Modified from Upchurch *et al.*, 2004:character number 146)

(183) Middle and posterior dorsal vertebrae, neural canal in anterior view: entirely surrounded by the neural arch (0); enclosed in a deep fossa, enclosed laterally by pedicels (1). (Upchurch *et al.*, 2004:character number 136)

(184) Middle and posterior dorsal vertebrae, neural spine height: approximately twice the centrum length (0); for times the centrum length (1). (Upchurch *et al.*, 2004)

(185) Middle and posterior dorsal neural spines orientation: vertical (0); slightly inclined, with an angle of around 70 degrees (1); strongly inclined, with an angle not bigger than 40 degrees (2). (Modified from Wilson, 2002:character number 104)

(186) Middle and posterior dorsal vertebral, central keel: absent (0); present (1). (D'Emic, 2012:character number 49)

(187) Dorsal vertebrae, height of the neural arch divided the height of the centrum: less than 0.8 (0); more than 0.8 (1). (Pol et al., 2011:character number 132)

(188) Middle to posterior dorsal vertebrae, pleurocoel dorsal margin: rounded (0); angular (1). (Rauhut et al. 2015:character number 346)

(189) Middle to posterior dorsal vertebrae, pleurocoel dorsal margin: well below the dorsal margin of the centrum (0); at the level of the dorsal margin of the centrum or higher (1). (Rauhut et al., 2015:character number 347)

(190) Middle to posterior dorsal vertebrae, small fossa anterior or anteroventral to the pleurocoel: absent (0); present (1). (Rauhut et al. 2015:character number 348)

(191) Middle and posterior dorsal neural arches, centropostzygapophyseal lamina (CPOL), shape: simple (0); divided (1). (Wilson, 2002:character number 95)

(192) Middle and posterior dorsal neural arches, anterior centroparapophyseal lamina (ACPL): absent (0); present (1). (Wilson, 2002:character number 96; Upchurch *et al.*, 2004:character number 133)

(193) Middle and posterior dorsal neural arches, prezygoparapophyseal lamina (PRPL): absent (0); present (1). (Wilson, 2002:character number 97)

(194) Middle and posterior dorsal neural arches, posterior centroparapophyseal lamina (PCPL): absent (0); present (1). (Wilson, 2002:character number 98, Upchurch *et al.*, 2004:character number 137)

(195) Middle and posterior dorsal centrum in transverse section (height: width ratio): subcircular (ratio, similar to 1 or a bit higher) (0); slightly dorsoventrally compressed (ratios between 0.8 and 1) (1); strongly compressed (ratios below 0.8) (2). (Modified from Upchurch *et al.*, 2004)

(196) Middle and posterior dorsal vertebrae neural spine, triangular aliform processes: absent (0); present but do not project far laterally (not as far as caudal zygapophyses) (1); present and project far laterally (as far as caudal zygapophyses) (2). (Modified from Wilson, 2002:character number 102 and Upchurch *et al.*, 2004:chs. 153-154).

(197) Middle and posterior dorsal vertebrae, spinodiapophyseal lamina (SPDL): absent (0); present (1). (Upchurch *et al.*, 2004:character number 157)

(198) Middle and posterior dorsal vertebrae, accessory spinodiapophyseal lamina (SPDL): absent (0); present (1). (Upchurch *et al.*, 2004:character number 151)

(199) Dorsal vertebrae, spinodiapophyseal webbing: lamina follows curvature of neural spine in anterior view (0); lamina "festooned" from spine, dorsal margin does not closely follow shape of neural spine and diapophysis (1). (Whitlock, 2011:character number104)

(200) Anterior dorsal vertebrae, spinopostzygapophyseal lamina (SPOL): absent (0); present (1). (Upchurch *et al.*, 2007:character number133)

(201) Middle and posterior dorsal neural spines, lateral spinopostzygapophyseal lamina (lSPOL): absent (0); present (1). (Wilson, 2002: 100; Upchurch *et al.*, 2004:character number 159)

(202) Middle and posterior dorsal neural arches, spinodiapophyseal lamina (SPDL) and spinopostzygapophyseal lamina (lSPOL) contact: absent (0); present (1). (Wilson, 2002:character number 101)

(203) Middle and posterior dorsal vertebrae, spinodiapophyseal (SPDL) and spinopostzygapophyseal lamina (lSPOL) contact: ventral, well separated from the triangular aliform process (0); dorsal, forms part of the triangular aliform process (1). (Carballido et al., 2012)

(204) Middle and posterior dorsal vertebrae, height of neural arch below the postzygapophyses (pedicel): less than height of centrum (0); subequal to or greater than height of centrum (1). (Whitlock, 2011:character number 109)

(205) Posterior Dorsal vertebrae, medial spinopostzygapophyseal lamina (mSPOL): absent (0); present and forms part of the median posterior lamina (1). (Carballido et al., 2012)

(206) Posterior dorsal vertebrae, transverse processes: lie posterior, or posterodorsal, to the parapophysis (0); lie vertically above the parapophysis (1). (Upchurch *et al.*, 2004:character number 139)

(207) Posterior dorsal centra, articular face shape: amphicoelous (0); slightly opisthocoelous (1); opisthocoelous (2). (Modified from Wilson, 2002:character number 105)

(208) Posterior dorsal vertebrae, neural spine: narrower transversely than anteroposteriorly (0); broader transversely than anteroposteriorly (1). (Wilson, 2002: character number 92)

(209) Posterior dorsal vertebra, posterior centrodiapophyseal lamina (PCDL): has an unexpanded ventral tip (0); expands and may bifurcate toward its ventral tip (1). (Salgado *et al.*, 1997)

(210) Cervical ribs, distal shafts of longest cervical ribs: are elongate and form overlapping bundles (0); are short and do not project beyond the caudal end of the centrum to which they are attached (1). (Wilson, 2002:character number 140)

(211) Cervical ribs, angle between the capitulum and tuberculum: greater than 90°, so that the rib shaft lies close to the ventral edge of the centrum (0); less than 90°, so that the rib shaft lies below the ventral margin of the centrum (1). (Wilson, 2002:character number 139)

(212) Dorsal ribs, proximal pneumatopores: absent (0); present (1). (Wilson, 2002:character number 141)

(213) Anterior dorsal ribs, cross-sectional shape: subcircular (0); plank-like, anteroposterior breadth more than three times mediolateral breadth (1). (Wilson, 2002).

Sacrum

(214) Sacral vertebrae, number:: 3 or fewer (0); 4 (1); 5 (2); 6 (3). (Wilson, 2002:character number 108)

(215) Sacrum, sacricostal yoke: absent (0); present (1). (Wilson, 2002:character number 109)

(216) Sacral vertebrae contributing to acetabulum: numbers 1-3 (0); numbers 2-4 (1). (Wilson, 2002:character number 110)

(217) Sacral neural spines length: approximately twice length of centrum (0); approximately four times length of centrum (1). (Wilson, 2002:character number 111)

(218) Sacral ribs, dorsoventral length: low, not projecting beyond dorsal margin of ilium (0); high extending beyond dorsal margin of ilium (1). (Wilson, 2002:character number 112)

(219) Pleurocoels in the lateral surfaces of sacral centra: absent (0); present (1). (Upchurch *et al.*, 2004:character number 165)

Caudal vertebrae

(220) Caudal vertebrae, number: 35 or fewer (0); 40 to 55 (1); increased to 70-80 (2). (Wilson, 2002:character number114)

(221) Caudal bone texture: solid (0); spongy (camellate), with large internal cells (1). (Wilson, 2002:character number 113)

(222) Anterior caudals, pneumatized neural arch: absent (0); present (1).

(223) Caudal transverse processes: persist through caudal 20 or more posteriorly (0); disappear by caudal 15 (1); disappear by caudal 10(2). (Wilson, 2002:character number 115)

(224) First caudal centrum anterior articular surface: flat (0); concave (1); convex (2).

(225) First caudal centrum, posterior articular surface: flat (0); concave (1); convex (2).

The first caudal vertebra of *Patagotitan* has an unusual morhology having a flat anterior articulation surface and a markedly convex posterior one. Therefore, the character reflecting the first caudal centrum morphology (platycoelous, procoelous or biconvex) was split in two characters, one for the anterior articular surface and the second one for the posterior articular surface morphology.

(226) First caudal neural arch, coel on lateral aspect of neural spine: absent (0); present (1). (Wilson, 2002:character number 117)

(227) Anterior caudal vertebrae (mainly the first and second): ventral bulge on transverse process: absent (0); present (1). (D'Emic, 2012:character number 52)

(228) Anterior and middle caudal vertebrae, blind fossae in lateral centrum: absent (0); present (1). (D'Emic, 2012:character number 56)

(229) Posteriormost anteriors and middle caudal vertebrae, transverse processes orientation: perpendicular (0); swept backwards, reaching the posterior margin of the centrum (1). (D'Emic, 2012:character number 59)

(230) Anterior caudal vertebrae, transverse processes: ventral surface directed laterally or slightly ventrally (0); directed dorsally (1). (Whitlock, 2011:character number 125)

(231) Anterior caudal centra (excluding the first), articular face shape: amphiplatyan or amphicoelous (0); procoelous/distoplatyan (1); slightly procoelous (2); procoelous (3); posterior surface markedly more concave than the anterior one (4). (Modified from González Riga *et al*, 2009)

(232) Anterior caudal centra, pleurocoels: absent (0); present (1). (Wilson, 2002:character number 119)

(233) Anterior caudal vertebrae, ventral surfaces: convex transversely (0); concace transversely (1). (Upchurch *et al.*, 2004:character number 182)

(234) Anterior and middle caudal vertebrae, ventrolateral ridges: absent (0); present (1). (Upchurch *et al.*, 2004:character number 183)

(235) Anterior and middle caudal vertebrae, triangular lateral process on the neural spine: absent (0); present (1). (Whitlock, 2011:character number 123)

(236) Anterior caudal transverse processes shape: triangular, tapering distally (0); "wing-like", not tapering distally (1). (Wilson, 2002:character number 128)

(237) Anterior caudal neural spines, transverse breadth: approximately 50% of (0); or greater than anteroposterior length (1). (Wilson, 2002:character number 126)

(238) Anterior caudal transverse processes, proximal depth: shallow, on centrum only (0); deep, extending from centrum to neural arch (1). (Wilson, 2002:character number 127)

(239) Anterior caudal transverse processes, diapophyseal laminae (ACDl, PCDL, PRDL, PODL): absent (0); present (1). (Wilson, 2002:character number 129)

(240) Anterior caudal transverse processes, anterior centrodiapophyseal lamina (ACDL), shape: single (0); divided (1). (Wilson, 2002:character number 130)

(241) Anterior caudal vertebrae, hyposphene ridge: absent (0); present (1). (Upchurch *et al.*, 2004:character number 187)

(242) Anterior caudal centra, length: approximately the same (0); or doubling over the first 20 vertebrae (1). (Wilson, 2002:character number 120)

(243) Anterior caudal neural arches, spinoprezygapophyseal lamina (SPRL): absent, or present as small short ridges that rapidly fade out into the anterolateral margin of the spine (0); present, extending onto lateral aspect of neural spine (1); present, well developed and extending onto the anterior or anterolateral edges of the neural spine (2)(Modified from Wilson, 2002:character number 121). A third state was incorporated in order to include the morphology observed in some taxa in which the SPRL is well developed, but is not extending into the lateral aspect of the neural spine, as is the case of *Patagotitan*.

(244) Anterior caudal neural arches, spinodiapophyseal lamina (SPDL): absent (0); present (1). In titanosaurs the SPDL, when present, is extending from the dyapophyseal section of the transverse process (the dorsalmost part of it) up to the neural spine.

(245) Anterior caudal neural arches, spinoprezygapophyseal lamina (SPRL)-spinopostzygapophyseal lamina (SPOL) contact: absent (0); present, forming a prominent lamina on lateral aspect of neural spine (1). (Wilson, 2002:character number 122)

(246) Anterior caudal neural arches, prespinal lamina (PRSL): absent (0); present (1). (Wilson, 2002:character number 123)

(247) Anterior caudal vertebrae, ventral and medially placed SPRL, usually described as bifurcated PRSL: absent (0); present (1). This character was originally proposed as an autapomorphy of *Futalognkosaurus* but is not just restricted to this sauropod.

(248) Anterior caudal prespinal lamina (PRSL), triangular shaped product of a dorsal expansion of it: absent (0); present (1).

(249) Anterior caudal vertebrae, pair thin laminae that are bounding the prespinal laminae and that diverge dorsally: absent (0); present (1). This character was initially proposed as an autapomorphy of *Bonitasuras* but is present in some other sauropods, such as *Patagotitan*.

(250) Middle caudal centra, shape: cylindrical (0); with flat ventral margin (1); quadrangular, flat ventrally and laterally (2). (Modified from Wilson, 2002:character number 131)

(251) Anterior and middle caudal centra, ventral longitudinal hollow: absent (0); present (1). (Wilson, 2002:character number 132)

(252) Middle caudal centra, articular face shape: amphiplatyan or amphicoelous (0); procoelous/distoplatyan (1); slightly procoelous (2); procoelous (3). (González Riga *et al.*, 2009)

(253) Posteriormost anteriors and iddle caudal vertebrae, location of the neural arches: over the midpoint of the centrum with approximately subequal amounts of the centrum exposed at either end (0); on the anterior half of the centrum (1). (Upchurch *et al.*, 2004:character number 185)

(254) Anterior caudal vertebrae, anterior face of the centrum strongly inclined anteriorly: absent (0); present (1). (Santucci and Arruda Campos, 2011: character number 256)

(255) Middle caudal vertebrae, with the anterior face strongly inclined anteriorly: absent (0); present (1).

(256) Middle caudal vertebrae, height of the pedicels below the prezygapophysis: low with curved anterior edge of the pedicel (0); high with vertical anterior edge of the pedicel (1). (Carballido et al., 2012)

(257) Middle caudal vertebrae, orientation of the neural spines: anteriorly (0); vertical (1); slightly directed posteriorly (2); strongly directed posteriorly (3). (Modified from Wilson, 2002:character number 133)

(258) Posterior caudal vertebrae, neural spine strongly displaced posteriorly: absent (0); present (1). (Carballido et al., 2012).

(259) Middle caudal vertebrae, ratio of centrum length to centrum height: less than 2, usually 1.5 or less (0); 2 or higher (1). (Upchurch *et al.*, 2004:character number 179)

(260) Anterior-posterior caudal vertebrae (those with still well developed neural spine) , neural spine orientation: vertical (0); slightly directed posteriorly (1); strongly directed posteriorly (2). (Carballido et al., 2012)

(261) Posterior caudal centra, articular face shape: anphyplatic (0); procoelous (1); opisthocoelous (2). (Modified from González Riga *et al.,* 2009)

(262) Posterior caudal centra, shape: cylindrical (0); dorsoventrally flattened, breadth at least twice height (1). (Wilson, 2002:character number 135)

(263) Posterior caudal vertebrae, ratio of length to height: less than 5, usually 3 or less (0); 5 or higher (1). (Upchurch *et al.*, 2004:character number 180)

(264) Distalmost caudal centra, articular face shape: platycoelous (0); biconvex (1). (Wilson, 2002:character number 136)

(265) Distalmost biconvex caudal centra, number: 10 or fewer (0); more than 30 (1). (Wilson, 2002:character number 137)

(266) Distalmost biconvex caudal centra, length-to height ratio: less than 4 (0); greater than 5 (1). (Wilson, 2002:character number 138)

(267) Forked chevrons with anterior and posterior projections: absent (0); present (1). (Wilson, 2002:character number 143)

(268) Forked chevrons, distribution: distal tail only (0); throughout middle and posterior caudal vertebrae (1). (Wilson, 2002:character number 144)

(269) Chevrons, crus bridging dorsal margin of haemal canal: present (0); absent (1). (Wilson, 2002:character number 145)

(270) Chevron haemal canal, depth: short, approximately 25% (0); or long, approximately 50% chevron length (1). (Wilson, 2002:character number 146)

(271) Chevrons: persisting throughout at least 80% of tail (0); disappearing by caudal 30 (1). (Wilson, 2002:character number 147)

(272) Posterior chevrons, distal contact: fused (0); unfused (open) (1). (Wilson, 2002:character number 148)

(273) Posture: bipedal (0); columnar, obligatory quadrupedal posture (1). (Wilson, 2002:character number 149)

Scapular girdle

(274) Scapular acromion process, size: Narrow (0); broad, width more than 150% minimum width of blade (1). (Wilson, 2002:character number 150)

(275) Scapular blade, orientation respect to coracoid articulation: perpendicular (0); forming a 45º angle (1). (Wilson, 2002:character number 151)

(276) Scapular blade, distal expansion: absent (0); present (1).
This character was introduced for recognizing those sauropods which scapular blade is not markedly expanded distally. The third state is recognized in several sauropods, such as *Patagotitan*, *Alamosaurus*, *Rinconsaurus*.

(277) Scapular blade, shape: acromial edge not expanded (both edges are running parallel to each other) (0); rounded expansion on acromial side (1); racquet-shaped (2): marked distal expansion due to the posterodorsal orientation of the dorsal edge (3). (Wilson, 2002:character number 152

The third state was added in order to incorporate the morphology observed in the scapular blade of *Patagotitan* and other sauropods in which the scapular is markedly expanded respect to the narrower section of the blade, and this expansion is due to the inclination of the dorsal edge.

(278) Scapula, acromion process dorsal margin: concave or straight (0); with V-shaped concavity (1); with U-shaped concavity (2). (Sereno *et al.*, 2007: 88)

(279) Scapula, highest point of the dorsal margin of the blade: lower than the dorsal margin of the proximal end (0); at the same height than the dorsal margin of the proximal end (1); higher than the dorsal margin of the proximal end (2). (Carballido et al., 2012 from Mannion, 2009)

(280) Scapula, development of the acromion process: undeveloped (0); well developed (1). (Carballido et al., 2012)

(281) Scapular length/minimum blade breadth: 5.5 or less (0); 5.5 or more (1). (Carballido et al., 2012)

(282) Scapula, ventral margin with a well-developed ventromedial process: absent (0); present (1). (Carballido et al., 2011)

(283) Scapular, acromial process position: lies nearly glenoid level (0); lies nearly midpoint scapular body (1). (Carballido et al., 2012)

(284) Scapular acromion length: less than 1/2 scapular length (0); at least 1/2 scapular length (1). (Mannion *et al.*, 168)

(285) Glenoid scapular orientation: relatively flat or laterally facing (0); strongly bevelled medially (1). (Wilson, 2002:character number 153)

(286) Scapular blade, cross-sectional shape at base: flat or rectangular (0); D-shaped (1). (Wilson, 2002:character number 154)

(287) Coracoid, proximodistal length: less than the length of scapular articulation (0); approximately twice the length of scapular articulation (1). (Wilson, 2002:character number 155)

(288) Coracoid, anteroventral margin shape: rounded (0); rectangular (1). (Wilson, 2002:character number 156)

(289) Dorsal margin of the coracoid in lateral view: reaches or surpasses the the level of the dorsal margin of the scapular expansion (0); lies below the level of the scapular proximal expansion and separated from the latter by a V-shaped notch (1). (Upchurch *et al.,* 2004:character number 207)

(290) Coracoid, Infraglenoid deep groove: absent (0); present (1).

(291) Coracoid, infraglenoid lip: absent (0); present (1). (Wilson, 2002:character number 157)

(292) Sternal plate, shape: posterolateral margin curved (0); posterolateral margin expanded as a corner (1). (D'Emic, 2012:character number 76)

(293) Sternal plate, shape: oval (0); crescentic (1). (Wilson, 2002:character number 158)
(294) Prominent posterolateral expansion of the sternal plate producing a kidney-shaped profile in dorsal view: absent (0); present (1). (Upchurch *et al.,* 2004:character number211)
(295) Prominent parasagital oriented ridge on the dorsal surface of the sternal plate: absent (0); present (1). (Upchurch *et al.,* 2004: :character number212)
(296) Ridge on the ventral surface of the sternal plate: absent (0); present (1). (Upchurch *et al.,* 2004:character number213)
(297) Ratio of maximum length of sternal plate to the humerus length: less than 0,75, usually less than 0,65 (0); greater than 0,75 (1). (Upchurch *et al.*, 2004:character number209)

Fore limbs
(298) Humerus, strong posterolateral bulge around the level of the deltopectoral crest: absent (0); present (1). (D'Emic, 2012:character number 80)
(299) Humerus, radial and ulnar condyles shape: radial condyle divided on anterior face by a notch (0); undivided (1). (D'Emic, 2012:character number 83)
(300) Humerus-to-femur ratio: less than 0.60 (0); 0.60 to 0.90 (1); greater than 0.90 (2). (Upchurch *et al.*, 2004:character number 216)
(301) Humeral deltopectoral attachment, development: prominent (0); reduced to a low crest or ridge (1). (Wilson, 2002:character number160)
(302) Humeral deltopectoral crest, shape: relatively narrow throughout length (0); markedly expanded distally (1). (Wilson, 2002:character number161)
(303) Humeral midshaft cross-section, shape: circular (0); elliptical (1). (Mannion *et al*, 2011:character number 170)
(304) Humerus, RI (*sensu* Wilson and Upchurch, 2003): Gracile (less than 0,27) (0); medium (0,28-0,32) (1); Robust (more than 0,33) (2). (Carballido et al., 2012)
(305) Humeral distal condyles, articular surface shape: restricted to distal portion of humerus (0); exposed on anterior portion of humeral shaft (1). (Wilson, 2002:character number 163)
(306) Humeral distal condyle, shape: divided (0); flat (1). (Wilson, 2002:character number 164)
(307) Humeral, lateral margin: medially deflected (0); almost straight until the half length or even more (1); almost straight until the proximal third of the total length of the humerus (2). (Carballido et al., 2012)
(308) Humeral proximolateral corner, shape: rounded, the dorsal surface is well convex (0); pronounced / square, the dorsal surface low, almost flat (1). (Wilson, 2002:character number 159)
(309) Ulnar proximal condyle, shape: subtriangular (0); triradiate, with deep radial fossa (1). (Wilson, 2002character number 165)
(310) Ulnar proximal condylar processes, relative lengths: subequal (0); unequal, anterior arm longer (1). (Wilson, 2002:character number 166)
(311) Ulnar olecranon process, development: prominent, projecting above proximal articulation (0); rudimentary, level with proximal articulation (1). (Wilson, 2002:character number 167)

(312) Ulna, length-to-proximal breadth ratio: gracile (0); stout (1). (Wilson, 2002:character number 168)

(313) Radial distal condyle, shape: round (0); subrectangular, flattened posteriorly and articulating in front of ulna (1). (Wilson, 2002:character number 169)

(314) Radius, distal breadth: slightly larger than midshaft breadth (0); approximately twice midshaft breadth (1). (Wilson, 2002:character number170)

(315) Radius, distal condyle orientation: perpendicular to long axis of shaft (0); bevelled approximately 20º proximolaterally relative to long axis of shaft (1). (Wilson, 2002:character number171)

(316) Carpal bones, number: 3 or more (0); 2 or fewer (1). (Wilson, 2002:character number173)

(317) Carpal bones, shape: round (0); block-shaped, with flattened proximal and distal surfaces (1). (Wilson, 2002:character number174)

(318) Metacarpus, shape: spreading (0); bound, with sub-parallel shafts and articular surfaces that extend half their length (1). (Wilson, 2002:character number175)

(319) Metacarpals, shape of proximal surface in articulation: gently curving, forming a 90arc (0); U-shaped, subtending a 270arc (1). (Wilson, 2002:character number176)

(320) Longest metacarpal-to-radius ratio: close to 0.3 (0); 0.45 or more (1). (Wilson, 2002:character number177)

(321) Metacarpal I, length: shorter than metacarpal IV (0); longer than metacarpal IV (1). (Wilson, 2002:character number178)

(322) Metacarpal I, distal condyle shape: divided (0); undivided (1). (Wilson, 2002:character number 179)

(323) Metacarpal I distal condyle, transverse axis orientation: bevelled approximately 20º respect to axis of shaft (0); proximodistally or perpendicular with respect to axis of shaft (1). (Wilson, 2002:character number 180)

(324) Manual digits II and III, phalangeal number: 2- 3-4-3-2 or more (0); reduced, 2-2-2-2-2 or less (1); absent or unossified (2). (Wilson, 2002:character number 181)

(325) Manual phalanx I.1, shape: rectangular (0); wedge-shaped (1). (Wilson, 2002:character number 182)

(326) Manual nonungual phalanges, shape: longer proximodistally than broad transversely (0); broader transversely than long proximodistally (1). (Wilson, 2002:character number 183)

Pelvic girdle

(327) Pelvis, anterior breadth: narrow, ilia longer anteroposteriorly than distance separating preacetabular processes (0); broad, distance between preacetabular processes exceeds anteroposterior length of ilia (1). (Wilson, 200:character number 1842)

(328) Ilium, ischial peduncle size: large, prominent (0); low, rounded (1). (Wilson, 2002:character number 185)

(329) Ilium, dorsal margin shape: flat (0); semicircular (1). (Wilson, 2002:character number 186)

(330) Illium, preacetabular process, kink on ventral margin: absent (0); present (1). (D'Emic, 2012:character number 99)

(331) Ilium, preacetabular process shape: pointed, arching ventrally (0); semicircular, with posteroventral excursion of cartilage cap (1). (Wilson, 2002:character number 188)

(332) Ilium, preacetabular process orientation: anterolateral to body axis (0); perpendicular to body axis (1). (Wilson, 2002:character number 189)

(333) Highest point on the dorsal margin of the ilium: lies caudal to the base of the pubic process (0); lies cranial to the base of the pubic process (1). (Upchurch *et al.*, 2004:character number 245)

(334) Pubis length respect to ischium: pubis slightly smaller or subequal to ischium (0); pubis larger (120% +) than ischium (1). (Carballido et al., 2012)

(335) Pubis, ambiens process development: small, confluent with anterior margin of pubis prominent, (0); projects anteriorly from anterior margin of pubis (1). (Wilson, 2002:character number 189)

(336) Pubic apron, shape: flat (straight symphysis) (0); canted anteromedially (gentle S-shaped symphysis) (1). (Wilson, 2002:character number 190).

(337) Puboischial contact, length: approximately one third total length of pubis (0); one-half total length of pubis (1). (Wilson, 2002:character number 191)

(338) Ischium, acetabular articular surface: maintains approximately the same transverse width throughout its length (0); is transversely narrower in its central portion and strongly expanded as it approaches the iliac and pubic articulations (1). (Mannion *et al.*, 2013:character number 180)

(339) Ischium, iliac peduncle with constriction or "neck": absent (0); present (1). (Whitlock, 2011:character number 173).

(340) Ischium, elongate muscle scar on proximal end: absent (0); present (1). (Whitlock, 2011:character number 174)

(341) Ischial blade, shape: emarginate distal to pubic peduncle (0); no emargination distal to pubic peduncle (1). (Wilson, 2002:character number 193)

(342) Ischia pubic articulation: less or equal to the anteroposterior length of pubic pedicel (0); greater than the anteroposterior length of pubic pedicel (1). (Salgado *et al.*, 1997)

(343) Ischia, anteroposterior pubic pedicel width divided the total length of the ischium: less than 0.5 (0); 0.5 or larger (1). (Carballido et al., 2012).

(344) Ischial distal shaft, shape: triangular, depth of ischial shaft increases medially (0); bladelike, medial and lateral depths subequal (1). (Upchurch *et al.*, 2004:character number 194)

(345) Ischial distal shafts, cross-sectional shape: V-shaped, forming an angle of nearly 50º with each other (0); flat, nearly coplanar (1). (Wilson, 2002:character number 195)

(346) Ischia, distal end: is only slightly expanded (0); is strongly expanded dorsoventrally (1). (Upchurch, 1998:character number 183)

(347) Ichium, angle formed between the shaft and the acetabular line: forming an almost right angle (80-110°) (0) or; a close angle (less than 70°) (1). (Carballido et al., 2012)

(348) Ischial tuberosity: absent (0); present (1).

The tuberosity, noted by Otero (2010) for the ischium of *Neuqunesaurus* (Otero, 2010:Fig. 8) and is present in other taxa, such as *Patagotitan*, *Bonitasaura*, *Futalognkosaurus*, *Alamosaurus* and *Neuquensaurus*.

Hind limbs

(349) Femur, longitudinal ridge on the anterior face: absent (0); present (1). (D'Emic, 2012:character number 107)

(350) Femur, fibular condyle: well developed, having a similar height than the tibial one (0); much shorter than the tibial condyle (1).

The fibular condyle of *Patagotitan* and *Bonitasaura* is reduced in its posterior projection respect to that of most other sauropods, which fibular and tibial condyles are almost equally posteriorly projected.

(351) Femur, epicondyle development: well developed (0); reduced, almost absent (1).

In *Patagotitan* the epicondyle is extremely developed and notorious in posterior and distal view, as a minor step laterally projected. In contrast in some titanosaurs the epicondyle is almost imperceptible, as is the case of *Dreadnoughtus*, *Opsithocoelicaudia*, *Neuqunesaurus* and *Saltasaurus*.

(352) Femur, fourth trochanter position: almost at the half of the femur (0); in the proximal third of the femur (1).

The fourth trochanter of *Patagotitan* is positioned around the proximal third of the total femur length, similar to the position observed in *Futalognkosaurus*, *Bonitasaura*, and some other non-*Lognkosauria* as *Rapetosaurus*, *Saltasaurus* and *Neuquensaurus*. In contrast the fourth trochanter of most sauropods is around the half of the total femur length, being even some more lower in *Opisthocoelicaudia.*

(353) Femur, fourth trochanter development: prominent (0); reduced to crest or ridge (1); extremely reduced (2). (Modified from Wilson, 2002:character number 196, following to Whitlock, 2011:character number 186)

(354) Femur, lesser trochanter: present (0); absent (1). (Wilson, 2002:character number 197)

(355) Femur midshaft, transverse diameter: subequal to anteroposterior diameter (0); 125-150% anteroposterior diameter (1); at least 185% anteroposterior diameter (2). (Wilson, 2002:character number 198)

(356) Femur, lateral bulge (marked by the lateral expansion and a dorsomedial orientation of the laterodorsal margin of the femur, which starts below the femur head ventral margin): absent (0); present (1). (Salgado *et al.*, 1997)

(357) Femur, pronounced ridge on posterior surface between greater trochanter and head: absent (0); present (1). (Whitlock, 2011:character number 181)

(358) Femur head position: perpendicular to the shaft, rises at the same level than the greater trochanter (0); dorsally directed, rises well above the level of the greater trochanter (1). (Modified from Upchurch *et al.*, 2004:character number 263)

(359) Femur, distal condyles relative transverse breadth: subequal (0); tibial much broader than fibular (1). (Wilson, 2002:character number 2000)

(360) Femur, distal condyles orientation: perpendicular or slightly bevelled dorsolaterally (0); or beveled dorsomedially approximately 10 relative to femoral shaft (1). (Wilson, 2002:character number 201)

(361) Femur, distal condyles articular surface shape: restricted to distal portion of femur (0); expanded onto anterior portion of femoral shaft (1). (Wilson, 2002:character number 202)

(362) Situation of the femoral fourth trochanter: on the caudal surface of the shaft, near the midline (0); on the caudomedial margin of the shaft (1). (Upchurch *et al.*, 2004:character number 268)

(363) Tibial proximal condyle, shape: narrow, long axis anteroposterior (0); expanded transversely, condyle subcircular (1). (Wilson, 2002:character number 203)

(364) Tibial cnemial crest, orientation: projecting anteriorly (0); or laterally (1). (Wilson, 2002:character number 204)

(365) Tibia, distal breadth: approximately 125% (0); more than twice midshaft breadth (1). (Wilson, 2002:character number 205)

(366) Tibial distal posteroventral process, size: broad transversely, covering posterior fossa of astragalus (0); shortened transversely, posterior fossa of astragalus visible posteriorly (1). (Wilson, 2002:character number 206)

(367) Fibula, proximal tibial scar, development: not well-marked (0); well-marked and deepening anteriorly (1). (Wilson, 2002:character number 207)

(368) Fibula, lateral trochanter: absent (0); present (1). (Wilson, 2002:character number 208)

(369) Fibular distal condyle, size: subequal to shaft (0); expanded transversely, more than twice midshaft breadth (1). (Wilson, 2002:character number 209)

(370) Fibular, proximal end, anterior crest: absent or poorly developed (0); well developed creating an interlocking proximal crus (1). (D'Emic, 2012:character number 111)

(371) Fibula, shaft shape: straight, or slightly sigmoidal (0); sigmoid, such that the proximal and distal faces are angled relative to midshaft (1). (D'Emic, 2012:character number 113)

(372) Astragalus, shape: at least 1.5 times wider than anteroposteriorly long (0); anteroposterior and transverse dimensions subequal (1). (D'Emic, 2012:character number 115)

(373) Astragalus, shape: rectangular (0); wedge shaped, with reduced anteromedial corner (1). (Wilson, 2002:character number210)

(374) Astragalus, fibular facet: faces laterally (0); faces posterolaterally, anterior margin visible in posterior view (1). (Whitlock, 2011:character number 186)

(375) Astragalus, foramina at base of ascending process: present (0); absent (1). (Wilson, 2002:character number 211)

(376) Astragalus, ascending process length: limited to anterior two-thirds of astragalus (0); extending to posterior margin of astragalus (1). (Wilson, 2002:character number 212)

(377) Astragalus, posterior fossa shape: undivided (0); divided by vertical crest (1). (Wilson, 2002:character number 213)

(378) Astragalus, transverse length: 50% more than (0); or subequal to proximodistal height (1). (Wilson, 2002:character number 214)

(379) Calcaneum: present (0); absent or unossified (1). (Wilson, 2002:character number 215)

(380) Distal tarsals 3 and 4: present (0); absent or unossified (1). (Wilson, 2002:character number 216)

(381) Metatarsus, posture: bound (0); spreading (1). (Wilson, 2002:character number 217)

(382) Metatarsal I proximal condyle, transverse axis orientation: perpendicular to (0); angled ventromedially approximately 15º to axis of shaft (1). (Wilson, 2002:character number 218)

(383) Metatarsal I distal condyle, transverse axis orientation: perpendicular to (0); angled dorsomedially to axis of shaft (1). (Wilson, 2002:character number 219)

(384) Metatarsal III length divided by metatarsal I length: less than 1.3 (0); more than 1.3 (1). (González Riga et al., 2016:character number 331)

(385) Longest metatarsal: metatarsal III (0); metatarsal IV (1). (González Riga et al., 2016:character number 334)

(386) Metatarsal I distal condyle, posterolateral projection: absent (0); present (1). (Wilson, 2002:character number 220)

(387) Metatarsal I, minimum shaft width: less than that of metatarsals II-IV (0); or greater than that of metatarsals IIIV (1). (Wilson, 2002:character number 221)

(388) Metatarsal I and V proximal condyle, size: smaller than (0); or subequal to those of metatarsals II and IV (1). (Wilson, 2002:character number 222)

(389) Metatarsal III length: more than 30% (0); or less than 25% that of tibia (1). (Wilson, 2002:character number 223)

(390) Metatarsals III and IV, minimum transverse shaft diameters: subequal to (0); or less than 65% that of metatarsals I or II (1). (Wilson, 2002:character number 224)

(391) Metatarsal IV, proximomedial end, shape: flat or slightly concave (0); possesses a distinct embayment (1). (D'Emic, 2012:character number 117)

(392) Metatarsal IV, distal end, orientation: roughly perpendicular to long axis of bone (0); bevelled upwards medially (1). (D'Emic, 2012:character number 118)

(393) Metatarsal V, length: shorter than (0); or at least 70% length of metatarsal IV (1). (Wilson, 2002:character number 225)

(394) Pedal nonungual phalanges, shape: longer proximodistally than broad transversely (0); broader transversely than long proximodistally (1). (Wilson, 2002:character number 226)

(395) Pedal digits II-IV, penultimate phalanges, development: subequal in size to more proximal phalanges (0); rudimentary or absent (1). (Wilson, 2002:character number 227)

(396) Pedal unguals, orientation: aligned with (0); or deflected lateral to digit axis (1). (Wilson, 2002:character number 228)

(397) Pedal digit I ungual, length relative to pedaldigit II ungual: subequal (0); 25% larger than that of digit II (1). (Wilson, 2002:character number 229)

(398) Pedal digit I ungual, length: shorter (0); or longer than metatarsal I (1). (Wilson, 2002:character number 230)

(399) Pedal ungual I, shape: broader transversely than dorsoventrally (0); sickle-shaped, much deeper dorsoventrally than broad transversely (1). (Wilson, 2002:character number 231)

(400) Pedal ungual II-III, shape: broader transversely than dorsoventrally (0); sickle-shaped, much deeper dorsoventrally than broad transversely (1). (Wilson, 2002:character number 232)

(401) Pedal digit IV ungual, development: subequal in size to unguals of pedal digits II and III (0); rudimentary or absent (1). (Wilson, 2002:character number 233)

(402) Unguals of pedal digit II and III, proximal dimensions: as broad as deep (0); significantly broader than deep (1). (Allain and Aquesbi, 2008:character number 253)

(403) Number of phalanges in pedal digit II: 3 (0); 2 (1). (González Riga et al., 2016:character number 348)

(404) Number of phalanges in pedal digit III: 4 (0); 3 (1). (González Riga et al., 2016:character number 349)

(405) Number of phalanges in pedal digit IV: 3 or more (0); 2 (1); 1 (2). (González Riga et al., 2016:character number 350)

Additional references

Alexander, R. M. (1989). Dynamics of dinosaurs and other extinct giantes (Vol. 194). New York: Columbia University Press. doi:10.1038/194632c0

Anderson, J. F. (1985). Long-bone circumference and weight in mammals, birds and dinosaurs. *J . Zool., Lond. (A)*, *207*, 53–61. doi:10.1111/j.1469-7998.1985.tb04915.x

Apesteguía, S. (2004). *Bonitasaura salgadoi gen. et sp. nov.:* A beaked sauropod from the Late Cretaceous of Patagonia. *Naturwissenschaften*, *91*(10), 493–497. doi:10.1007/s00114-004-0560-6

Bates, K. T., Falkingham, P. L., Macaulay, S., Brassey, C., & Maidment, S. C. R. (2015). Downsizing a giant: re-evaluating *Dreadnoughtus* body mass. *Biology Letters*, *11*(6), 20150215. http://doi.org/10.1098/rsbl.2015.0215

Bates, K. T. et al. (2016). Temporal and phylogenetic evolution of the sauropod body plan. *Royal Society Open Science*, 3:150636. doi: 10.1098/rsos.150636

Benson, R. B. J., Campione, N. E., Carrano, M. T., Mannion, P. D., Sullivan, C., Upchurch, P., & Evans, D. C. (2014). Rates of Dinosaur Body Mass Evolution Indicate 170 Million Years of Sustained Ecological Innovation on the Avian Stem Lineage. *PLoS Biology*, *12*(5), e1001853. http://doi.org/10.1371/journal.pbio.1001853

Bonaparte, J. F., & Coria, R. A. (1993). Un Nuevo y gigantesco sauropodo titanosaurio de la Formación Rio Limay (Albiano-Cenomaniano) de la Provincia del Neuquén, Argentina. *Ameghiniana*, *30*, 271–282.

Bonaparte. J. F. & Powell, J. E. (1980). A continental assemblage of tetrapods from the Upper Cretaceous of Northwestern Argentina (Sauropoda-Coelurosauria-Carnosauria-Aves). *Mémoires de la Société Géologique de France*, 139, 19-28

Borsuk-bialynicka, M. (1977). A New Camarasaurid Sauropod *Opisthocoelicaudia skarzynskii gen. n., sp.* n. from the Upper Cretaceous of Mongolia. *Paleontologia Polonica*, *37*, 5–64.

Bowring, J. F., McLean, N. M., & Bowring, S. A. (2012). Engineering cyber infrastructure for U-Pb geochronology: Tripoli and U-Pb-Redux. *Geochemistry, Geophysics, Geosystems*, *12*(6). oi:10.1029/2010GC003479

Calvo, J. O., González-Riga, B. J., & Porfiri, J. D. (2007). A new titanosaur sauropod from the Cretaceous of Neuquén, Patagonia, Argentina. *Arquivos Do Museu Nacional*, *65*(4), 485–504.

Calvo, J. O., & González Riga, B. J. (2003). *Rinconsaurus caudamirus gen. et sp. nov*., a new titanosaurid (Dinosauria, Sauropoda) from the Late Cretaceous of Patagonia, Argentina. *Revista Geológica de Chile*, *30*(2), 1–24. doi:10.4067/S0716-02082003000200011

Calvo, J.O. & Bonaparte, J.F. (1991). *Andesaurus delgadoi gen. et sp. nov*. (Saurischia-Sauropoda), dinosaurio Titanosauridae de la Formacion Rio Limay (Albiano-Cenomaniano), Neuquén, Argentina. *Ameghiniana ,* 28: 303-310.

Calvo, J. O., Porfiri, J. D., González-Riga, B. J., & Kellner, A. W. A. (2007). A new Cretaceous terrestrial ecosystem from Gondwana with the description of a new sauropod dinosaur. *Anais Da Academia Brasileira de Ciencias*, *79*(3), 529–541. doi:10.1590/S0001-37652007000300013

Calvo, J. O., Coria, R. A., & Salgado, J. L. (1997). Uno de los más completos Titanosauridae (Dinosauria - Sauropoda) registrados en el mundo. *Ameghiniana*, *34*, 534.

Campione, N. E., & Evans, D. C. (2012). A universal scaling relationship between body mass and proximal limb bone dimensions in quadrupedal terrestrial tetrapods. *BMC Biology*, *10*(1), 60. doi:1.1186/1741-7007-10-60

Cantino, P. D., & Queiroz, K. (2006). International Code of Phylogenetic Nomenclature.

Carballido, J. L., Pol, D., Parra Ruge, M. L., Padilla Bernal, S., Páramo-Fonseca, M. E., & Etayo-Serna, F. (2015). A new Early Cretaceous brachiosaurid (Dinosauria, Neosauropoda) from northwestern Gondwana (Villa de Leiva, Colombia). *Journal of Vertebrate Paleontology*, *35*(5), e980505. http://doi.org/10.1080/02724634.2015.980505

Carmona, R.P., Umazano, A.M., Krause, J.M. (2016) Estudio estratigráfico y sedimentológico de las sedimentitas portadoras de los titanosaurios gigantes del Albiano tardío de Patagonia Central, Argentina. *Latin American Journal of Sedimentology and Basin Analysis*, *23*, 127–132.

Chinsamy-Turan. (2005). *The microstructure of dinosaur bone*. Baltimore: Johns Hopkins University Press.

Chinsamy, A., & Raath, M. a. (1992). Preparation of fossil bone for histological examination. *Palaeontologia Africana*, *29*, 39–44.

Condon, D.J., Schoene, B., McLean, N.M., Bowring, S.A. & Parrish, R.R. 2015 Metrology and traceability of U-Pb isotope dilution geochronology (EARTHTIME Tracer Calibration Part I). *Geochimica Et Cosmochimica Acta* **164**, 464-480.

Coria, R. A., Filippi, L., Chiappe, L. M., Garcia, R., & Arcucci, A. B. (2013). *Overosaurus paradasorum gen. et sp. nov.,* a new sauropod dinosaur (Titanosauria: Lithostrotia) from the Late Cretaceous of Neuquén, Patagonia, Argentina. *Zootaxa*, *3683*(4), 357–376. doi:10.11646/zootaxa.3683.4.2

D'Emic, M. D. (2012). The early evolution of titanosauriform sauropod dinosaurs. *Zoological Journal of the Linnean Society*, *166*(3), 624–671. doi:10.1111/j.1096-3642.2012.00853.x

Fowler, D. W., & Sullivan, R. M. (2011). The First Giant Titanosaurian Sauropod from the Upper Cretaceous of North America. *Acta Palaeontologica Polonica*, *56*(4), 685–690. doi:10.4202/app.2010.0105

Francillon-Vieillot, et al. (1990). Microstructure and Mineralization of vertebrate skeletal tissues. In *Skeletal Biomineralization: Patterns, Processes and Evolutionary Trends* (Vol. l, pp. 471–530). CHAP, American Geophysical Union. doi:10.1029/SC005p0175

Franco-Rosas, A. C., Salgado, L., Rosas, C. F., & Carvalho, I. D. S. (2004). Nuevos materiales de titanosaurios (sauropoda) en el cretacico superior de mato groso, brasil. *Revista Brasileira de Paleontologia*, *7*(3), 329–336.

Gallina, P. A., & Otero, A. (2015). Reassessment of *Laplatasaurus araukanicus* (Sauropoda: Titanosauria) from the Upper Cretaceous of patagonia, Argentina. *Ameghiniana*, *52*(5), 487–501. doi:10.5710/AMGH.08.06.2015.2911

Gallina, P. A. & Apesteguía, S. (2011). Cranial anatomy and phylogenetic position of the titanosaurian sauropod *Bonitasaura salgadoi*. *Acta Palaeontologica Polonica* 56, 45–60.

Gallina, P. A., & Apesteguía, S. (2015). Postcranial anatomy of *Bonitasaura salgadoi* (Sauropoda, Titanosauria) from the Late Cretaceous of Patagonia. *Journal of Vertebrate Paleontology*, e924957. doi: 10.1080/02724634.2014.924957

Gilmore, C. W. (1936). Osteology of *Apatosaurus*, with special reference to specimens in the Carnegie Museum. *Memoirs of the Carnegie Museum*, 4, 172–209.

Gilmore, C. W. (1946). Reptilian fauna of the North Horn Formation of central Utah. *United States Geological Survey Professional Paper*, *201–C*, 29–53.

González Riga, B. J., & David, L. O. (2014). A new titanosaur (Dinosauria, Sauropoda) from the Upper Cretaceous (Cerro Lisandro Formation) of Mendoza Province, Argentina. *Ameghiniana*, *51*(1), 3–25. doi:10.5710/AMEGH.26.12.1013.1889

González Riga, B. J., Lamanna, M. C., Ortiz David, L. D., Calvo, J. O., & Coria, J. P. (2016). A gigantic new dinosaur from Argentina and the evolution of the sauropod hind foot. *Scientific Reports*, *6*, 19165. doi:10.1038/srep19165

González Riga, B. J., Previtera, E., & Pirrone, C. A. (2009). *Malarguesaurus florenciae gen. et sp. nov.,* a new titanosauriform (Dinosauria, Sauropoda) from the Upper Cretaceous of Mendoza, Argentina. *Cretaceous Research*, *30*(1), 135–148. doi:10.1016/j.cretres.2008.06.006

Grellet-Tinner, G., & Fiorelli, L. E. (2010). A new Argentinean nesting site showing neosauropod dinosaur

Jacobs, L. L., Winkler, D. a, Downs, W. R., & Gomani, E. M. (1993). New material of an early Cretaceous titanosaurid sauropod dinosaur from Malawi. *Palaeontology*. Retrieved from http://www.scopus.com/inward/record.url?eid=2-s2.0-0027799861&partnerID=40

Jaffey, A. H., Flynn, K. F., Glendenin, L. E., Bentley, W. C., & Essling, A. M. (1971). Precision measurement of half-lives and specific activities of U235 and U238. *Physical Review C*, *4*(5), 1889–1906. doi:10.1103/PhysRevC.4.1889

Kellner, W., Campos, D., & Trotta, M. N. F. (2005). Description of a titanosaurid caudal series from the Bauru Group, Late Cretaceous of Brazil. *Arquivos Do Museu Nacional, Rio de Janeiro*, *63*(3), 529–564.

Kellner, A. W. A., and S. A. K. Azevedo. 1999. A new sauropod dinosaur (Titanosauria) from the Late Cretaceous of Brazil. Pp. 111–142 in Y. Tomida, T.H. Rich and P. Vickers-Rich (eds.), Proceedings of the Second Gondwana Symposium, Tokyo, October 1999. National Science Museum Monographs 15.

Klein, N. & Sander, P.M. (2008). Ontogenetic stages in the long bone histologyof sauropod dinosaurs. *Paleobiology* 34: 248–264.

Lacovara, K. J., et al. (2014). A Gigantic, Exceptionally Complete Titanosaurian Sauropod Dinosaur from Southern Patagonia, Argentina. *Scientific Reports*, *4*, 6196. doi:10.1038/srep06196

Lu, J. C., Xu, L., Jia, S. H., Zhang, X. L., Zhang, J. M., Yang, L. L., … Ji, Q. (2009). A new gigantic sauropod dinosaur from the Cretaceous of Ruyang, Henan, China. *Geological Bulletin of China*, *28*(1), 1–10.

Maddison, W. P., & Maddison, W. P. (2016). Mesquite: a modular system for evolutionary analysis. Retrieved from http://mesquiteproject.org

Mattinson, J. M. (2005). Zircon U-Pb chemical abrasion ("CA-TIMS") method: Combined annealing and multi-step partial dissolution analysis for improved precision and accuracy of zircon ages. *Chemical Geology*, *220*(1–2), 47–66. http://doi.org/10.1016/j.chemgeo.2005.03.011

Mazzetta, G. V., Christiansen, P., & Fariña, R. a. (2004). Giants and Bizarres: Body Size of Some Southern South American Cretaceous Dinosaurs. *Historical Biology: A Journal of Paleobiology*, *16*(2–4), 71–83. http://doi.org/10.1080/08912960410001715132

McLean, N.M., Condon, D.J., Schoene, B. & Bowring, S.A. 2015 Evaluating uncertainties in the calibration of isotopic reference materials and multi-element isotopic tracers (EARTHTIME Tracer Calibration Part II). *Geochimica Et Cosmochimica Acta* **164**, 481-501.

McLean, N. M., Bowring, J. F., & Bowring, S. A. (2011). An algorithm for U-Pb isotope dilution data reduction and uncertainty propagation. *Geochemistry, Geophysics, Geosystems*, *12*(6). http://doi.org/10.1029/2010GC003478

Navarrete, C., Casal, G., & Martínez, R. (2011). Drusilasaura deseadensis gen. et sp. nov., un nuevo titanosaurio (dinosauria-sauropoda), de la formación bajo barreal, cretácico superior del norte de Santa Cruz, Argentina. *Revista Brasileira de Paleontologia*, *14*(1), 1–14. http://doi.org/10.4072/rbp.2011.1.01

Novas, F. E., Salgado, L., Calvo, J., & Agnolin, F. (2005). Giant titanosaur (Dinosauria, Sauropoda) from the Late Cretaceous of Patagonia. *Revista Del Museo Argentino de Ciencias Naturales*, *7*(1), 37–41.

Ogg, J.G. & Hinnov, L.A. 2012 Cretaceous. In *The Geological time scale 2012* (eds. F.M. Gradstein, J.G. Ogg, M.D. Schmitz & G.M. Ogg), pp. 793-853. Amsterdam, Elsevier.

Pol, D., & Escapa, I. H. (2009). Unstable taxa in cladistic analysis: identification and the assessment of relevalnt characters. *Cladistics*, *25*(5), 515–527. http://doi.org/10.1111/j.1096-0031.2009.00258.x

Powell, J.E. 1987. The Late Cretaceous fauna of Los Alamitos, Patagonia, Argentina. Part VI. The titanosaurids. *Revista del Museo Argentino de Ciencias Naturales "Bernardino Rivadavia"* 3: 147-153.

Ramezani, J., Hoke, G.D., Fastovsky, D.E., Bowring, S.A., Therrien, F., Dworkin, S.I., Atchley, S.C. & Nordt, L.C. 2011. High-precision U-Pb zircon geochronology of the Late Triassic Chinle Formation, Petrified Forest National Park (Arizona, USA): Temporal constraints on the early evolution of dinosaurs. *Geological Society of America Bulletin*, **123**, 2142-2159, http://doi.org/10.1130/b30433.1.

Rasband, W. (2016). Image J. Retrieved from http://rsb.info.nih.gov/ij/.

Salgado, L., Gallina, P. a., & Paulina Carabajal, A. (2015). Redescription of *Bonatitan reigi* (Sauropoda: Titanosauria), from the Campanian–Maastrichtian of the Río Negro Province (Argentina). *Historical Biology*, *27*(5), 525–548 doi:10.1080/08912963.2014.894038

Salgado, L. (2003). Should we abandon the name titanosauridae?: some commentrs on the taxonomy of titanosaurian sauropods (Dinosauria). *Revista Española de Paleontologíaola de Paleontologia*, *18*(1), 15–21.

Salgado, L., Coria, R. A., & Calvo, J. O. (1997). Evolution of titanosaurid sauropods. I: Phylogenetic analysis based on the postcranial evidence. *Ameghiniana*, *34*(1), 3–32.

Salgado, L., & García, R. A. (2002). Variación morfológica en la secuencia de vértebras caudales de algunos saurópodos titanosaurios. *Ameghiniana*, *17*(17), 211–216.

Salgado, L., & Powell, J. E. (2010). Reassessment of the vertebral laminae in some South American titanosaurian sauropods. *Journal of Vertebrate Paleontology*, *30*(6), 1760–1772. doi:10.1080/02724634.2010.520783

Santucci, R. M., & De Arruda-Campos, A. C. (2011). A new sauropod (Macronaria, Titanosauria) from the Adamantina Formation, Bauru Group, Upper Cretaceous of Brazil and the phylogenetic relationships of Aeolosaurini. *Zootaxa*, *33*(3085), 1–33.

Sanz, J. L., Powell, J. E., Loeuff, J. Le, Martinez, R., & Pereda-Suberbiola, X. (1999). Sauropod remains from the Upper Cretaceous of Laño (north central Spain). Titanosaur phylogenetic relationships. *Estudios Del Museo de Ciencias Naturales de Alava*, *14*(1), 235–255.

Sellers, W. I., Hepworth-Bell, J., Falkingham, P. L., Bates, K. T., Brassey, C. a., Egerton, V. M., & Manning, P. L. (2012). Minimum convex hull mass estimations of complete mounted skeletons. *Biology Letters*, *8*(5), 842–845. doi:10.1098/rsbl.2012.0263

Suárez, M., Márquez, M., De La Cruz, R., Navarrete, C., & Fanning, M. (2014). Cenomanian-? Early Turonian minimum age of the Chubut Group, Argentina: SHRIMP U-Pb geochronology. *Journal of South American Earth Sciences*, *50*, 67–74. doi:10.1016/j.jsames.2013.10.008

Upchurch, P., Barrett, P. M., & Dodson, P. (2004). The Dinosauria. In D. B. Weishampel, P. Dodson, & H. Osmólska (Eds.), *The Dinosauria* (University, pp. 259–322). Berkley: University of California Press.

Wedel, M. J., Cifelli, R. L., & Sanders, R. K. (2000). Sauroposeidon proteles, a new sauropod from the Early Cretaceous of Oklahoma. *Journal of Vertebrate Paleontology*, *20*(1), 109–114. doi:10.1671/0272-4634(2000)020[0109:SPANSF]2.0.CO;2

Wilson, J. A., & Upchurch, P. (2003). A revision of Titanosaurus Lydekker (Dinosauria - Sauropoda), the first dinosaur genus with a "Gondwanan" distribution\n. *Journal of Systematic Palaeontology*, *1*(3), 125–160. doi:10.1017/S1477201903001044

You, H. L. & Li, D. Q. (2009). The first well-preserved Early Cretaceous brachiosaurid dinosaur in Asia. Proceedings of the Royal Society. doi: 10.1098/rspb.2009.1278